STEM CELLS®

EMBRYONIC STEM CELLS/INDUCED PLURIPOTENT STEM CELLS

An Efficient Nonviral Method to Generate Integration-Free Human-Induced Pluripotent Stem Cells from Cord Blood and Peripheral Blood Cells

KEISUKE OKITA,[a] TATSUYA YAMAKAWA,[a] YASUKO MATSUMURA,[a] YOSHIKO SATO,[a] NAOKI AMANO,[a] AKIRA WATANABE,[a] NAOKI GOSHIMA,[b] SHINYA YAMANAKA[a,c,d,e]

[a]Department of Reprogramming Science, Center for iPS Cell Research and Application (CiRA), and [c]Institute for Integrated Cell-Material Sciences, Kyoto University, Kyoto, Japan; [b]Biomedicinal Information Research Center, National Institute of Advanced Industrial Science and Technology, Tokyo, Japan; [d]Yamanaka iPS Cell Project, Japan Science and Technology Agency, Kawaguchi, Japan; [e]Gladstone Institute of Cardiovascular Disease, San Francisco, California, USA

Key Words. Induced pluripotent stem cells • Reprogramming • Plasmid • Peripheral blood • T cells • Cord blood

ABSTRACT

The generation of induced pluripotent stem cells (iPSCs) provides the opportunity to use patient-specific somatic cells, which are a valuable source for disease modeling and drug discovery. To promote research involving these cells, it is important to make iPSCs from easily accessible and less invasive tissues, like blood. We have recently reported the efficient generation of human iPSCs from adult fibroblasts using a combination of plasmids encoding OCT3/4, SOX2, KLF4, L-MYC, LIN28, and shRNA for *TP53*. We herein report a modified protocol enabling efficient iPSC induction from CD34$^+$ cord blood cells and from peripheral blood isolated from healthy donors using these plasmid vectors. The original plasmid mixture could induce iPSCs; however, the efficiency was low. The addition of EBNA1, an essential factor for episomal amplification of the vectors, by an extra plasmid greatly increased the efficiency of iPSC induction, especially when the induction was performed from $\alpha\beta$T cells. This improvement enabled the establishment of blood-derived iPSCs from seven healthy donors ranging in age from their 20s to their 60s. This induction method will be useful for the derivation of patient-specific integration-free iPSCs and would also be applicable to the generation of clinical-grade iPSCs in the future. STEM CELLS *2013;31:458–466*

Disclosure of potential conflicts of interest is found at the end of this article.

INTRODUCTION

Pluripotency can be induced with a combination of a few defined factors in somatic cells [1–3]. The generation of induced pluripotent stem cells (iPSCs) provides an opportunity to develop and use patient-specific somatic cells like neurons, cardiomyocytes, and beta islet cells, which are otherwise difficult to obtain. These cells make it possible to examine the cause(s) and mechanism(s) underlying various diseases in vitro. Disease-specific iPSCs have already been established for Huntington's disease, Parkinson's disease, spinal muscular atrophy, and Rett syndrome [4, 5].

Human iPSCs can be generated from a wide spectrum of somatic cells, including fibroblasts, keratinocytes, and mesenchymal stem cells in adipose tissue [2, 6, 7]. Among them, cord blood cells and peripheral blood mononuclear cells (PMNCs) are attractive sources to use for the generation of iPSCs because of the low invasiveness of their collection. For instance, local anesthesia, suture, and suture removal are necessary for isolation of fibroblasts by skin biopsy but not for blood isolation. In addition, cord blood banks have already collected large repertories of human leukocyte antigen haplotypes, which can become a source for histocompatible iPSC stocks. The induction of iPSCs from human peripheral blood cells was first reported by Loh et al. in 2009 [8]. They used retrovirus vectors for gene delivery and infected them into mobilized CD34$^+$ blood cells isolated from a donor after a 3-day injection of granulocyte colony stimulating factor. Although effective, this method is relatively labor-intensive and places a major burden on the donor, thus making it difficult to use as a conventional tool. In addition, retrovirus integration disrupts the endogenous genomic organization and might influence the in vitro disease modeling. To overcome these issues, Seki et al. used a nonintegrating virus vector,

Author contributions: K.O.: conception and design, financial support, collection and/or assembly of data, provision of study material, data analysis and interpretation, manuscript writing, and final approval of manuscript; T.Y.: collection and/or assembly of data, data analysis and interpretation, and manuscript writing; Y.M. and Y.S.: collection and/or assembly of data and provision of study material; N.A. and A.W.: collection and/or assembly of data and data analysis and interpretation; N.G.: provision of study material; S.Y.: conception and design, financial support, and manuscript writing.

Correspondence: Keisuke Okita, V.M.D., Ph.D., Department of Reprogramming Science, Center for iPS Cell Research and Application (CiRA), Kyoto University, 53 Kawahara-cho, Shogoin, Sakyo-ku, Kyoto 606-8507, Japan. Telephone: 81-75-366-7042; Fax: 81-75-366-7098; e-mail: okita-g@cira.kyoto-u.ac.jp Received May 29, 2012; accepted for publication November 7, 2012; first published online in STEM CELLS *EXPRESS* November 29, 2012. 1066-5099/2012/$30.00/0 doi: 10.1002/stem.1293

using the Sendai virus, as a tool for iPSC induction [9]. They isolated mononuclear cells from peripheral blood and stimulated the expansion of T cells with an anti-CD3 antibody and IL-2. The T cells were then used for the Sendai virus infection to generate iPSCs. Their vectors had temperature-sensitive mutations in the RNA genome. These mutations allowed Sendai virus amplification in the T cells and maintenance of transgene expression when the cells were cultured at the permissive temperature (37°C). After the establishment of iPSCs, the Sendai virus vectors could be removed by culturing the cells at the nonpermissive temperature (38°C), although the elimination needs to be experimentally confirmed. However, this method uses an infectious virus, which requires special care, particularly when it encodes oncogenic genes like C-MYC, and it is difficult to modify reprogramming factors and vector sequences in conventional laboratories because they lack the equipment and facilities for handling such viruses.

Episomal plasmids were also used for the deviation of nonintegrating iPSCs [10]. The widely used vectors have two components of the Epstein-Barr virus, OriP and EBNA1. The EBNA1 sequence encodes a protein and expresses it from its viral promoter after transduction into human somatic cells. The EBNA1 protein in turn recognizes the OriP sequence and induces plasmid amplification coincident with DNA amplification of the host cell. This system enables relatively high and long-term expression of the reprogramming factors. Yu et al. generated a combination of three plasmids, pEP4EO2SEN2K, pEP4EO2SET2K, and pCEP4-M2L (here called the T1 mix), which encode OCT3/4, SOX2, KLF4, c-MYC, NANOG, LIN28, and SV40 Large T antigen, and showed iPS induction from cord blood cells [11]. Chou et al. established iPSCs from PMNCs with their plasmids, pEB-C5 and pEB-Tg (termed C1), containing OCT3/4, SOX2, KLF4, c-MYC, LIN28, and SV40 Large T antigen, but not NANOG [12]. However, to the best of our knowledge, iPSC induction from peripheral blood with plasmid vectors is still inefficient.

We have recently reported an efficient combination of plasmids for human iPSC induction from fibroblasts, which encode OCT3/4, SOX2, KLF4, L-MYC, LIN28, and a shRNA for *TP53* [13]. We herein report a highly efficient method of iPSC induction from PMNCs using these plasmid vectors, with slight modification. We were able to establish hundreds of iPSCs from 1×10^6 PMNCs isolated from healthy donors ranging in age from their 20s to their 60s. The iPSCs had genomic rearrangement at the TRB and TRD loci, indicating their T-cell origin. We also established iPSCs that did not show any evidence of genomic rearrangement in the TRB, TRD, and IGH loci by changing the culture medium. Most of these iPSCs were integration-free, karyotypically normal, and effectively differentiated into various cell types in vivo. This represents a reliable method to generate patient-specific iPSCs and would be applicable for the generation of clinical-grade iPSCs in the future.

Materials and Methods

Cell Culture

Peripheral blood was obtained from healthy donors whose written informed consent was obtained in accordance with the institutional review board guidelines. $CD34^+$ cord blood cells were obtained from the Stem Cell Resource Network in Japan (Banks at Miyagi, Tokyo, Kanagawa, Aichi, and Hyogo) through the RIKEN BioResource Center (Tsukuba, Ibaraki, Japan, http://www.brc.riken.jp/inf/en/index.shtml). Human fibroblasts, HDF1388, were purchased from Cell Applications, Inc (San Diego, CA, http://www.cellapplications.com/). Human fibroblasts were cultured in Dulbecco's modified Eagle's medium (DMEM) (Nacalai Tesque, Kyoto, Japan, http://www.nacalai.co.jp/english/index.html) supplemented with 10% fetal bovine serum (FBS, Invitrogen, Carlsbad, CA, http://www.invitrogen.com/site/us/en/home.html). Human embryonic stem cell (ESC) lines (KhES-1 and KhES-3) were obtained from Kyoto University (Kyoto, Japan, http://www.nbrp.jp/). H1 and H9 were from WiCell Research Institute (Madison, WI, http://www.wicell.org/). Mouse embryonic fibroblasts (MEF) were isolated from day 13.5 embryos of C57BL/6 mice. MEF and SNL cells [14] were cultured in DMEM supplemented with 7% FBS, 2 mM L-glutamine, and 50 units and 50 mg/ml of penicillin and streptomycin, respectively. Established iPSCs and ESCs were maintained on mitomycin C-treated SNL cells in Primate ESC medium (ReproCELL, Yokohama, Kanagawa, Japan, http://www.reprocell.com/en/) containing 4 ng/ml of basic fibroblast growth factor (bFGF) (Wako, Osaka, Osaka, Japan, http://www.wako-chem.co.jp/english/) as described previously [15].

Vector Construction

Efficient gene expression was achieved by inserting the woodchuck hepatitis post-transcriptional regulatory element upstream of the polyadenylation signal of pCX-EGFP [16]. Its SV40-ori sequence was removed by BamHI digestion. The modified vector was then digested with EcoRI and was ligated with the EBNA1 coding region, which was amplified by PCR from pCEP4 (Invitrogen). This vector was designated "pCXWB-EBNA1." The coding regions or genomic fragments of NANOG, TERT, SALL4, ESRRB, TBX3, GLIS1, mir-302s, Wnt3a, cyclinD1, Utf1, and SV40LT were amplified by PCR. The fragments were then cloned into pENTR-D/TOPO (Invitrogen) and were recombined with pCXLE-gw by a LR reaction (Invitrogen), which has a Gateway cassette, rfC.1 (Invitrogen), into the EcoRI site of the pCXLE plasmid [13]. We also constructed a red fluorescent protein expression vector, pCXLE-DsRed, and a *TP53* shRNA expression vector, pCXLE-DsRed-shp53, to use as controls. The episomal vectors described by Yu et al. [10] and Chou et al. [12] were obtained from Addgene (#20924, 20925, 20926, 20927, 28213, and 28220; Cambridge, MA, http://www.addgene.org/).

Generation of iPSCs from PMNCs with Episomal Vectors

PMNCs were purified by density gradient centrifusion with Ficoll-paque Plus (GE Healthcare, Waukesha, WI, http://www3.gehealthcare.com/en/Global_Gateway) or BD Vacutainer CPT (BD Biosciences, Franklin Lakes, NJ, http://www.bdbiosciences.com) according to the manufacturer's instructions. Three micrograms of expression plasmid mixture was electroporated into $3–5 \times 10^6$ PMNCs with the Nucleofector 2b Device (Lonza, Basel, Switzerland, http://www.lonza.com/) with an Amaxa Human T-cell Nucleofector kit according to the manufacturer's instructions. The program used was V-24. The cell viability and transfection efficiency of PMNCs in our lab were 70%–80% and 40%–60%, respectively. The plasmid mixtures used in the experiments are shown in Supporting Information Table 1. The cells equivalent to $3 \times 10^4–1 \times 10^6$ of input cells were then seeded onto six-well plates covered with a MEF feeder layer. For the induction from $\alpha\beta$T cells, the transfected cells were cultured in X-vivo10 (Lonza) supplemented with 30 U/ml IL-2 (PeproTech Inc., Rocky Hill, NJ, http://www.peprotech.com/) and 5 μl/well of Dynabeads Human T-activator CD3/CD28. For non-T-cell induction, αMEM medium containing 10% FBS, 10 ng/ml IL-3, 10 ng/ml IL-6, 10 ng/ml G-CSF, and 10 ng/ml GM-CSF was used. Two days after the transfection, an equal volume of Primate ESC medium containing bFGF and 10 μM Y27632 was added into each well without aspiration of the previous medium. The culture medium was then replaced with Primate ESC medium containing bFGF and Y27632 4 days after the transfection. The colonies were counted 16–25 days after plating, and the colonies similar to human ESCs were selected for further cultivation and

evaluation. Generation of iPSC from $CD34^+$ rich population was performed as described previously with slight modification [17]. Briefly, purified $CD34^+$ cells from PMNC was expanded for 6 days in StemSpan SFEM medium (StemCell Technologies Inc, Vancouver, BC, Canada, http://www.stemcell.com) supplemented with 10 ng/ml IL-3, 100 ng/ml IL-6, and 300 ng/ml of Flt3 ligand, stem cell factor (SCF), and TPO. Three micrograms of the plasmid mixture was then electroporated into 1×10^5 cells. The cells equivalent to $0.2–6 \times 10^4$ of input cells were then seeded onto six-well plates coated with Retronectin (Takara Bio Inc., Otsu, Shiga, Japan, http://www.takara.co.jp) in the StemSpan medium. The culture medium was gradually changed to the Primate ESC medium as described above. The iPSC clones used in this study are summarized in Supporting Information Table 2. We calculated the iPSC induction efficiency based on the number of iPSC colonies per number of seeded cells which were estimated from the number of cells used for the electroporation.

Generation of iPSCs from Cord Blood $CD34^+$ Cells with Episomal Vectors

The frozen $CD34^+$ cells were thawed and cultured in αMEM medium containing 10% FBS, 50 ng/ml IL-6, 50 ng/ml sIL-6R, 50 ng/ml SCF, 10 ng/ml TPO, 20 ng/ml Flt3 ligand, and 20 ng/ml IL-3 for a few days before transfection. Three micrograms of expression plasmid mixtures was then electroporated into $5–40 \times 10^5$ $CD34^+$ cells with a Nucleofector 2b Device using an Amaxa Human $CD34^+$ cell Nucleofector kit according to the manufacturer's instructions. The program used was U-08. The cells were then cultured for 2 or 5 days, and $0.5–35 \times 10^4$ cells were replated onto 100 mm dishes covered with an SNL or MEF feeder layer. Equal volumes of αMEM medium containing cytokines and Primate ESC medium containing bFGF and 10 μM Y27632 were mixed and used for cultivation, followed by replacement with Primate ESC medium in 2 days. The colonies were counted 17–26 days after the transduction, and the colonies similar to human ESCs were selected for further cultivation and evaluation.

Characterization of iPSC Clones

The isolation of total RNA, RT-PCR of marker gene expression, DNA microarrays, episomal copy number detection, and teratoma formation were performed as previously described [13]. A Southern blot analysis was carried out as previously described [18]. PCR-based detection of the TRB rearrangement was performed with TCRB Gene Clonality Assay (InVivoScribe, San Diego, CA, http://www.invivoscribe.com/) according to the manufacturer's instructions. The chromosomal G-band analyses were performed at the Nihon Gene Research Laboratories (Sendai, Miyagi, Japan, http://www.ngrl-japan.com/index.html).

Exome Analysis

One microgram of genomic DNA was sheared with the Covaris E210 system and was subjected to exome enrichment using SeqCap EZ Exome Library v3.0 (Roche Diagnostics GmbH, Mannheim, Germany, http://www.roche-applied-science.com) according to the manufacturer's instructions. Illumina sequencing libraries were made by PCR with Illumina sequencing adaptors and were sequenced with HiSeq2000 (Illumina, Inc., San Diego, CA, http://www.illumina.com/). The sequenced reads were mapped to protein coding sequences of reference human genome (hg19) by BWA 0.6.2. Local realignment was performed around in/dels with the Genome Analysis Toolkit (GATK v1.6) [19]. Optical and PCR duplicates were marked in BAM files with Picard 1.68. Only the regions with over ×30 coverage observed in all samples were subjected to the following single nucleotide variation (SNV) call. Original HiSeq base quality scores were recalibrated with GATK TableRecalibration. SNVs were called with GATK UnifiedGenotyper and eliminate false-positive calls according to the Broad Institute's best-practice guidelines (Best Practice Variant Detection with the GATK v3, http://www.broadinstitute.org/gsa/wiki/index.php/Best_Practice_Variant_Detection_with_the_GATK_v3).

Statistical Analyses

Data are shown as the means ± SD. The statistical significance of differences between two groups was evaluated with the Wilcoxon signed-rank test.

Results

iPSC Generation from Cord Blood Cells

We have previously reported the establishment of plasmid-based vectors which can efficiently generate iPSCs from adult fibroblasts and dental pulp cells [13]. The most effective combination of reprogramming factors consists of OCT3/4, SOX2, KLF4, L-MYC, LIN28, and shRNA for *TP53*. We called this combination of plasmids Y4 (Supporting Information Table 1).

As the first step, we tried to generate iPSCs from $CD34^+$ cells isolated from cord blood with the Y4 combination (Fig. 1A). This population was enriched in hematopoietic stem cells and has been shown to possess the potential for reprogramming [20]. The frozen $CD34^+$ cells purified from two donors were cultured for a few days with cytokines, IL-3, IL-6, soluble IL-6 receptor, SCF, TPO, and Flt3 ligand. The Y4 mixture was then transduced by electroporation (Fig. 1A). The cells were recovered in the medium for a few days and replated onto feeder cells in a 1:1 mixture of human ESC medium and the medium containing cytokines. The mixed culture medium was then changed to the medium for human ESCs after 2 days. We added an inhibitor for Rho kinase to support the reprogramming process by inhibiting cell death [21].

The ESC-like colonies began to emerge 10 days after the plasmid transfection and were selected for expansion (Fig. 1B). The reprogramming efficiency was relatively high (up to 0.1%; Supporting Information Table 3). Both MEF and SNL feeder cells resulted in a similar colony number. Established clones formed flat and compacted colonies, and showed high nucleus-to-cytoplasm ratios, which were typical morphology of human ESCs (Fig. 1C). When injected into immunodeficient mice, the clones developed into teratomas, where they differentiated into various types of cells of all three germ layers, like neurons, gut-like epithelium, cartilage, and muscle (Fig. 1D--1F). Therefore, the Y4 mixture can induce iPSCs from $CD34^+$ cells derived from cord blood.

iPSC Generation from Peripheral Blood

We next attempted to carry out reprogramming from peripheral blood with the Y4 mixture. The experiments were performed with blood from a healthy Japanese donor (donor #1, male, 30s). After the isolation of peripheral blood, the fraction of PMNCs was separated by density gradient centrifusion, and 3 million cells were used for the plasmid transduction (Fig. 2A). The PMNCs were then directly plated into the culture dish covered with MEF feeder cells. PMNCs mainly consist of T lymphocytes, but also contain other cell types, such as B lymphocytes, monocytes, and macrophages. We used two different types of media for their cultivation. One medium contained IL-2 and antibodies against CD3 and CD28 to stimulate the proliferation of T cells. The other medium, termed non-T medium, was supplemented with FBS, IL-3, IL-6, G-CSF, and GM-CSF. The PMNCs were cultured in each of these media for 2 days. The media were then diluted with the same volume of ESC medium supplemented with bFGF and a Rock inhibitor, followed by complete replacement on day 4.

There was extensive cell proliferation from day 4 to day 10 in the T-cell-stimulating medium. A few tiny cell colonies

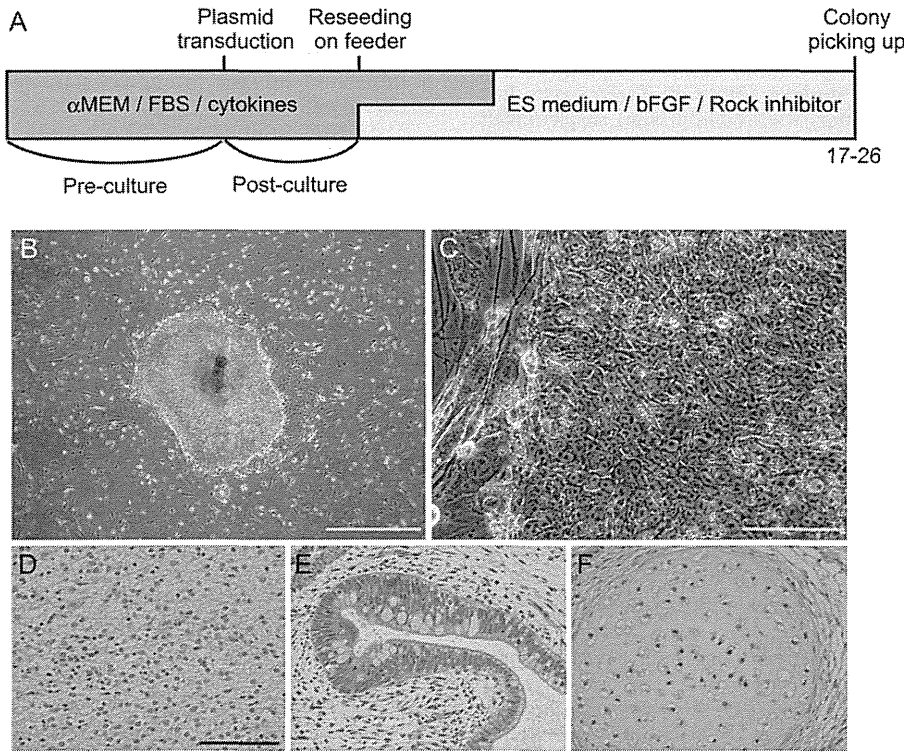

Figure 1. Establishment of human-induced pluripotent stem cells (iPSCs) from $CD34^+$ cord blood cells. **(A):** The iPSC induction protocol. Frozen $CD34^+$ cells were thawed and cultured in αMEM supplemented with FBS and cytokines. The cells were then transfected with the episomal vector mixture, followed by additional culture for 2–5 days, and were plated on six-well plates covered with feeder cells. The culture medium was gradually changed to ESC medium supplemented with bFGF and a Rock inhibitor. The iPSC colonies were counted and picked up for expansion around days 17–26. **(B, C):** Phase-contrast images of an iPSC colony and established cells. Bar = 1 mm in (B) and 50 μm in (C). **(D–F):** Teratoma formation. iPSCs derived from $CD34^+$ cord blood cells (clone 604B-1) were transplanted into immunodeficient mice. After 8 weeks, tumors were sectioned and stained with hematoxylin and eosin. Shown are neural tissues (D), gut-like epithelial tissues (E), and cartilage (F). Scale bar = 100 μm. Abbreviations: bFGF, basic fibroblast growth factor; ES, embryonic stem; FBS, fetal bovine serum.

firmly attached to the culture dish were observed around 2 weeks after the plasmid transduction. At this early time point, these cells showed a round morphology and clear cell-to-cell boundaries. Thereafter, these cells gradually adhered to each other and formed tightly packed colonies by 3 weeks. Conversely, obvious proliferation did not occur in the non-T medium. However, we were able to find colony formation with a similar time course as was observed with the T-cell-stimulating conditions. Around 3 weeks after the transduction, we counted the number of ESC-like colonies in the cultures under both conditions. In the medium for T-cell stimulation, 42.2 ± 8.4 colonies were obtained from 1×10^6 cells with the Y4 plasmid mixture (Fig. 2B; Table 1). Conversely, only 2.5 ± 1.0 colonies emerged from 1×10^6 cells in the non-T medium (Table 1). The established cells had morphology typical of human ESCs (Fig. 2C). A microarray analysis of gene expression revealed that they had a gene expression profile similar to that of ESCs (Supporting Information Table 4). Their linear correlation coefficient against ESCs (KhES3) was 0.993 on average, which is similar to the correlation coefficient of a different ESC line, H9, and fibroblast-derived iPSCs, 201B7 and 253G4, against KhES3 (R^2 = 0.991 and 0.988, respectively). The iPSCs showed the potential to differentiate into cells of all three germ layers by teratoma formation in mice (Fig. 2D-2F). Most of the iPSCs were karyotypically normal (Supporting Information Table 5).

Terminally differentiated αβT cells have genomic rearrangements in the TRB and TRA loci which encode the T-cell receptor (TCR) β and α chains, respectively. B cells have rearrangement in the immunoglobulin heavy locus, IGH. Therefore, we examined the cell origin of established iPSCs by detecting their genomic rearrangement by a Southern blot analysis. The iPS clones established under T-cell conditions (585A1, 585B1, 604A1, and 604B1) showed genomic rearrangement in TRB loci and did not show a specific band with the probe for the TRD locus (Fig. 2G; Supporting Information Fig. S1). The TRD locus is located within the TRA locus and is excised coincident with TRA rearrangement during the maturation of αβT cells. Hence, these data suggested that the four iPS clones were derived from αβT cells. In contrast, we could not detect any rearrangement of the three loci (TRB, TRD, and IGH) in iPS clones that developed in the non-T medium (692D2, 692E1, 648A1, and 648B1), thus indicating that they originated from nonlymphoid lineages.

We also tested other combinations of plasmids for PMNC reprogramming (Supporting Information Table 1). One combination, Y3, contains the same reprogramming factors as Y4 except for the shRNA against *TP53*. With the Y3 combination, iPSCs were obtained under both T-cell and non-T-cell conditions, but Y3 seemed to be less effective than Y4 (Table 1). We used other combinations of episomal plasmids which have been reported to induce iPSCs from blood cells [11, 12]. However, at least under our culture conditions, no iPSCs were obtained from PMNCs with T1 and C1 combinations (Table 1). We also used a combination, termed T2, containing the same reprogramming factors as T1, but contained them in two plasmids, pEP4EO2SCK2MEN2L and pEP4EO2SET2K [10]. Although the T2 combination could generate iPSCs from fibroblasts at better efficiency than T1 [13], we also failed to

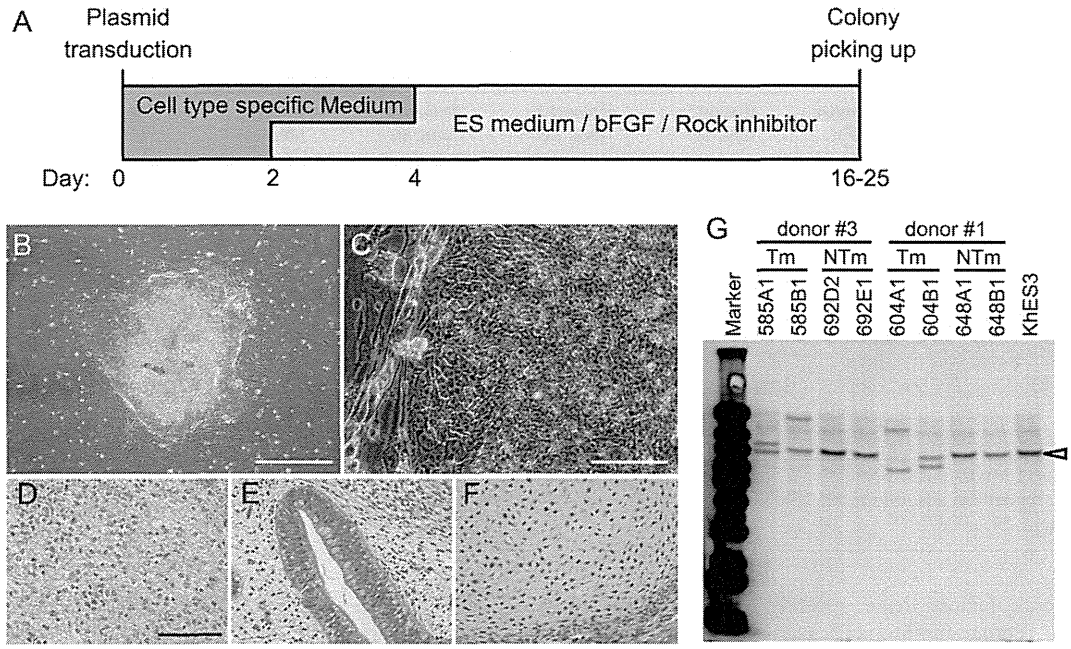

Figure 2. Establishment of human-induced pluripotent stem cells (iPSCs) from peripheral blood mononuclear cells (PMNCs). **(A):** The iPSC induction protocol. On day 0, PMNCs were isolated by gradient centrifusion, transfected with the episomal vector mixture, and were plated on six-well plates covered with MEF feeder cells. The cells were cultured in medium specific for different cell types. For example, the culture medium containing IL-2 and anti-CD3 and CD28 antibodies was used for T-cell stimulation. On day 2, the medium was diluted with the same volume of ESC medium supplemented with basic fibroblast growth factor and a Rock inhibitor, followed by complete replacement on day 4. iPSC colonies were counted and picked up for expansion around days 16–25. **(B, C):** Phase-contrast images of an iPSC colony (**B**) and an established iPSC (C). Bar = 1 mm in (B) and 50 μm in (C). **(D–F):** Teratoma formation. iPSCs (clone 604B1) were transplanted into immunodeficient mice. After 8 weeks, tumors were sectioned and stained with hematoxylin and eosin. Shown are neural tissues (D), gut-like epithelial tissues (E), and cartilage (F). Scale bar = 100 μm. **(G):** The results of the Southern blot analyses of the TRB locus. Genomic DNA (6 μg) was extracted from human ES cells (KhES3) and iPSCs, digested with Hind III, and analyzed for V(D)J rearrangements by a Southern blot analysis using a probe for the TRB locus. The open arrowheads indicate bands derived from the germline allele. The iPSCs were established in medium for non-T cells (NTm) or for T cells (Tm) from two different donors. The iPS clones (585A1, 585B1, 604A1, and 604B1) showed genomic rearrangement in the TRB locus. Abbreviation: ES, embryonic stem.

Table 1. Induced pluripotent stem cell induction efficiency from PMNCs obtained from donor #1

		Plasmid mixtures and conditions							
Medium[a]	Cell number ($\times 10^5$)	C1 ($n = 3$)	T1 ($n = 3$)	T2 ($n = 6$)	Y3 ($n = 3$)	Y3 + EBNA1 ($n = 3$)	Y4 ($n = 6$)	Y4 + EBNA1 ($n = 3$)	Y4 + EBNA1 with frozen PMNCs ($n = 3$)
NTm	10	0.0 ± 0.0	0.0 ± 0.0	0.0 ± 0.0	0.7 ± 0.6	1.3 ± 1.2	2.5 ± 1.0	4.7 ± 3.8	9.7 ± 2.1
	3	0.0 ± 0.0	0.0 ± 0.0	0.0 ± 0.0	0.0 ± 0.0	0.7 ± 0.6	0.7 ± 0.8	4.3 ± 2.1	2.3 ± 1.2
Tm	10	0.0 ± 0.0	0.0 ± 0.0	0.0 ± 0.0	15.7 ± 8.1	51.7 ± 64.4	42.2 ± 8.4	ND[b]	ND[b]
	3	0.0 ± 0.0	0.0 ± 0.0	0.0 ± 0.0	6.0 ± 3.5	9.0 ± 9.6	18.8 ± 6.1	184.0 ± 11.3	241.0 ± 77.7
	1	0.0 ± 0.0	0.0 ± 0.0	0.0 ± 0.0	2.7 ± 2.1	5.3 ± 3.1	9.5 ± 2.7	82.7 ± 11.6	101.0 ± 26.5
	0.3	0.0 ± 0.0	0.0 ± 0.0	0.0 ± 0.0	0.3 ± 0.6	0.7 ± 1.2	1.2 ± 0.8	19.3 ± 9.6	31.3 ± 12.9

[a]NTm, medium for non-T cell populations; Tm, medium for T cells.
[b]ND, not determined because too many colonies had formed.Abbreviation: PMNC, peripheral blood mononuclear cell.

induce iPSCs from PMNCs using T2 (Table 1). Thus, Y4 had the highest induction efficiency among the various plasmid combinations we tested.

We then examined whether Y4 could efficiently generate iPSCs from other donors (Table 2). PMNCs were isolated from six healthy male and female donors ranging in age from their 20s to their 60s, and induced reprogramming. However, the iPSC induction efficiency was different among the donors, and the efficiency of the six donors was relatively lower than that of donor #1. As described above, we could consistently obtain more than 25 iPSC colonies from 1×10^6 input cells from donor #1 when they were cultured under the T-cell condition. In contrast, only around five colonies emerged under the same conditions for donors #4 and #7. In addition, iPSC colonies were rarely obtained in the non-T-cell medium from the other donors. Two out of the three experiments failed to induce iPSC colonies from 1×10^6 input cells from donors #3, #4, and #7.

The Addition of an Extra EBNA1 Expression Vector Greatly Enhanced iPSC Formation from T Cells

In order to reproducibly generate iPSCs from T lymphocytes from multiple donors, it was necessary to improve our induction protocol. To this end, we took two approaches. First, we tried to improve the efficiency by means of proreprogramming

Table 2. iPS induction efficiency from 6 other donors

Factor	Medium[a]	Cell number ($\times 10^5$)	iPS colony number ($n = 3$) Donor#2 (20s, M)	Donor#3 (30s, M)	Donor#4 (40s, F)	Donor#5 (40s, M)	Donor#6 (40s, M)	Donor#7 (60s, M)
Y4	NTm	10	2.0 ± 1.0	0.3 ± 0.6	1.3 ± 2.3	2.0 ± 1.7	2.7 ± 0.6	0.7 ± 1.2
		3	0.7 ± 0.6	0.7 ± 0.6	0.0 ± 0.0	0.3 ± 0.6	1.0 ± 1.0	0.3 ± 0.6
	Tm	10	15.3 ± 1.5	6.3 ± 0.6	4.0 ± 1.7	17.3 ± 3.1	10.3 ± 5.7	5.0 ± 1.7
		3	7.7 ± 2.3	4.0 ± 2.0	3.3 ± 0.6	9.3 ± 3.5	2.7 ± 0.6	0.3 ± 0.6
		1	3.3 ± 2.1	1.3 ± 1.5	0.7 ± 0.6	6.0 ± 3.6	3.3 ± 1.5	2.3 ± 1.2
		0.3	1.0 ± 1.0	0.3 ± 0.6	0.7 ± 1.2	1.7 ± 2.1	0.0 ± 0.0	0.3 ± 0.6
Y4+EBNA1	NTm	10	3.3 ± 1.5	9.7 ± 4.2	3.3 ± 0.6	7.3 ± 1.2	6.3 ± 1.5	3.3 ± 0.6
		3	2.7 ± 0.6	4.0 ± 2.0	0.3 ± 0.6	2.7 ± 0.6	3.3 ± 3.2	1.0 ± 1.0
	Tm	10	ND[b]	ND[b]	116.7 ± 9.5	ND[b]	ND[b]	113.0 ± 19.1
		3	230.3 ± 15.2	113.0 ± 32.7	41.0 ± 10.4	192.7 ± 25.1	127.7 ± 19.4	27.0 ± 1.7
		1	100.3 ± 8.0	42.3 ± 15.5	21.3 ± 9.5	62.3 ± 19.5	47.3 ± 7.8	16.0 ± 7.0
		0.3	36.7 ± 22.9	10.7 ± 1.5	3.3 ± 2.1	20.0 ± 4.6	11.3 ± 2.5	6.7 ± 0.6

[a]NTm, medium for non-T cell populations; Tm, medium for T cells.
[b]ND, not determined because too many colonies formed. The donor age and sex are indicated.Abbreviations: F, female, iPS, induced pluripotent stem; M, male.

factors. Several factors have recently been reported to increase the reprogramming efficiency of human and/or mouse somatic cells using viral transduction methods [3, 22–31]. We cloned these 11 candidate genes into an episomal plasmid, transduced them one by one into human fetal dermal fibroblasts with the Y3 combination, and screened for their effects on the reprogramming efficiency. As expected, the addition of shRNA for *TP53* increased the number of iPSC colonies compared to Y3 alone; however, SALL4, TERT, Wnt3a, and Utf1 did not show any apparent influence on the reprogramming (Supporting Information Fig. S2A). Plasmids encoding ESRRB, TBX3, and SV40 large T antigen seemed to suppress iPSC induction. Conversely, transduction of NANOG, GLIS1, mir-302s, and cyclin D1 increased the number of iPSC colonies.

Notably, GLIS1 showed the highest enhancement of reprogramming, as it induced an approximately fourfold increase in the number of colonies compared to the control Y3 combination (Supporting Information Fig. S2A). GLIS1 also showed additional effects on *TP53* suppression and could generate twofold more iPSC colonies when used with the Y4 combination in fibroblasts (Supporting Information Fig. S2B). Based on these results, we expected that GLIS1 would enhance the iPSC induction from PMNCs. However, when cells were transduced with Y3 or Y4, the addition of GLIS1 showed only a slight or no increase in the number of iPSCs induced under both the T-cell and non-T-cell conditions (Fig. 3A, 3B). As a result, the proreprogramming effect of GLIS1 varies depending on the origin of the somatic cells.

As an alternative way to enhance the reprogramming efficiency, we aimed to increase the protein expression from our episomal plasmids. The maintenance of EBV-based plasmids is largely dependent on the EBNA1 protein. Previous reports have shown that a high transfection efficiency could be achieved by cell lines that constitutively express EBNA1 from an integrated genomic construct [32]. Based on this knowledge, we used an extra plasmid, pCXWB-EBNA1, encoding EBNA1 under the control of the CAG promoter (Supporting Information Fig. S3) [16]. To ensure early removal of the reprogramming plasmids, the additional vector did not include an OriP sequence, an essential component for episomal plasmid replication. Hence, the EBNA1 vector itself is not amplified in human cells and gives only a transient expression of EBNA1.

To examine the effect of this plasmid on the transgene expression, fibroblasts were transduced with episomal plasmids encoding EGFP in the presence and absence of the EBNA1 expression vector (Supporting Information Fig. S4). Six days after the transduction, enhanced green fluorescent protein (EGFP) fluorescence was analyzed by flow cytometry. The addition of EBNA1 greatly increased both the mean expression level and the population of $EGFP^+$ cells (from 8.5% to 17.2%). However, this high expression quickly diminished during cultivation. One month after the transduction, only 0.3% of cells remained positive for the fluorescence. Therefore, the transient expression of EBNA1 promoted amplification of the episomal vector at the early time points, but it had a minimal influence on the maintenance of the vectors in the later phase. Consistent with this result, the addition of the EBNA1 vector to the Y4 mix led to a twofold increase in the number of iPS colonies generated from fibroblasts (Supporting Information Fig. S5). The established clone, 923B1, showed expression of pluripotent genes similar to ESCs (Supporting Information Table 4). In addition, no obvious genomic integration was observed in the clones (Fig. 3C; Supporting Information Fig. S6).

We then performed iPS induction from PMNCs using this extra plasmid. The addition of the EBNA1 vector to the Y4 mixture increased the number of iPS colonies in seven different donors (Fig. 3D, 3E; Supporting Information Fig. S7; Tables 1 and 2). The Wilcoxon signed-rank test indicated that this modification led to a moderate but significant increase of the reprogramming under the non-T-cell conditions (median; 2.5-fold, $p < .05$) and achieved a dramatic enhancement of reprogramming in the cells cultivated under the T-cell culture conditions (median; 28-fold, $p < .05$, Fig. 3D). The reprogramming efficiency under the T-cell culture conditions was up to 0.1% at the maximum (Table 2). However, this was likely overestimated because of the vigorous expansion of transduced T cells before the initiation of the reprogramming and attachment to the culture plates. To assess whether this was the case, 15 iPS clones were randomly chosen from 31 colonies in one dish, and their genomic rearrangement pattern at the TRB locus was examined (Supporting Information Fig. S8). A Southern blot analysis and PCR-based detection revealed that two and three clones among these had an identical rearrangement pattern. Conversely, there were 12 different TRB rearrangements among 15 clones. These data suggested that some clones were derived from daughter cells of the

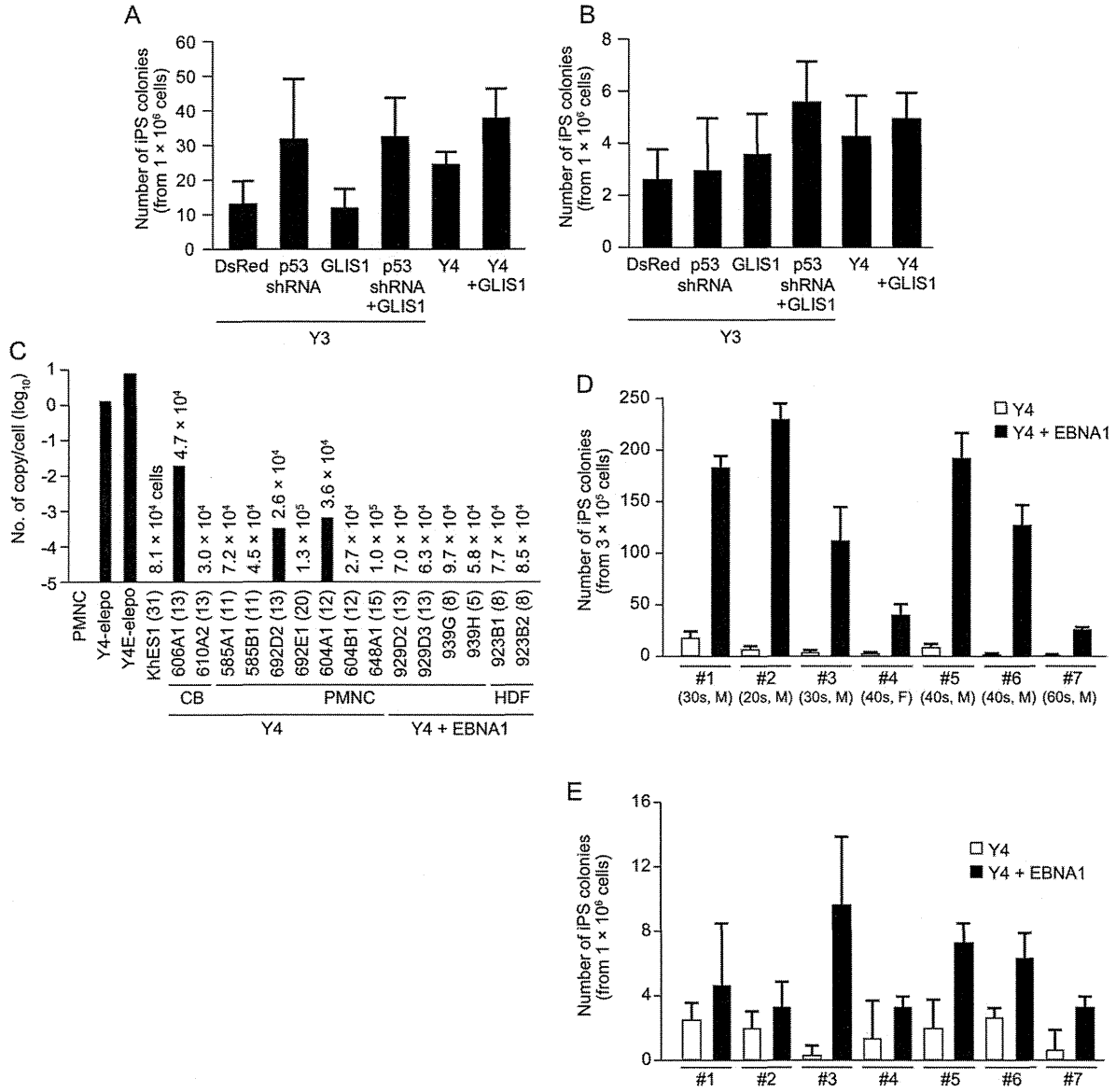

Figure 3. Improvement of the reprogramming efficiency by extra EBNA1. **(A, B):** The efficiency of iPSC generation from PMNCs cultured in the medium for T cells (A) and non-T cells (B) with GLIS1. The data are shown as the means ± SD of ESC-like colony numbers obtained from at least three independent experiments. **(C):** The copy numbers of episomal vectors that remained in the iPSC clones. The numbers in parentheses indicate the passage numbers of each clone. Also shown are the estimated numbers of cells analyzed for each clone. The PMNCs collected 4 days after electroporation of the Y4 (Y4-elepo) or Y4 plus EBNA1 vector (Y4E-elepo) combination were analyzed as positive controls. The tissue origin (CB, PMNC, and fibroblast [HDF]), and vectors used for iPSC induction are shown below. **(D, E):** The efficiency of iPSC generation from the PMNCs from seven donors in the medium for T cells (D) or non-T cells (E) with the additional EBNA1 vector. The donor number, age, and sex are indicated. Abbreviations: CB, cord blood; F, female; iPSC, induced pluripotent stem cell; M, male; PMNC, peripheral blood mononuclear cell.

same T cells, but that most of them were derived independently from different cells.

This induction method enabled the generation of more than 100 iPS clones from all of the donors we examined. The iPS clones induced with Y4 and the extra EBNA1 vector were isolated for a further analysis. The established clones (929D2 and 929D3) showed the expression of pluripotent genes, and no obvious genomic integration was found (Fig. 3C; Supporting Information Figs. S6 and S9; Table 4). They were karyotypically normal and had the potential to differentiate into various cell types of all three germ layers, indicating their pluripotency (Supporting Information Table 5; Fig. S10). When performed exome analysis, the numbers of nonsilent variations in iPSCs induced with Y4 and EBNA1 were 7 and 6 under the T-cell condition, and 1 and 6 under the non-T-cell conditions (Supporting Information Tables S6 and S7). These numbers were almost comparable with that observed in fibroblast-derived iPSCs [33]. The plasmid mixture could induce iPSCs from frozen PMNCs at almost the same efficiency as freshly isolated cells (Table 1). Moreover, when hematopoietic stem and progenitor cells were enriched from PMNCs by CD34 expression, the extra EBNA1 vector also enhanced iPSC generation (Supporting Information Table 8).

Discussion

T-cell-derived iPSCs have their own genomic rearrangements in TRB and TRA loci, which would prevent the generation of large repertories of TCR in redifferentiation towered T cells. Mice having successful prerearranged TCR were reported to show early TCR expression and aberrant T-cell development [34]. Therefore, T-cell-derived iPSCs would have some limitation in their use, such as clinical reconstitution of T lymphocytes and in vitro recapitulation of normal T-cell development.

The iPS induction was greatly enhanced when using the extra EBNA1 vector and the Y4 combination in the T-cell-stimulating medium. The proliferation of T cells can be activated by the combination of IL-2 and the stimulation of TCR complexes, along with costimulatory signaling via anti-CD3 and anti-CD28 antibodies [35]. The replication of EBV-based episomal vector occurs along with the host cell division. Therefore, cell proliferation is important for the maintenance of the episomal vectors in human cells. In addition, proliferation itself has been reported to increase the chance of fully reprogramming in a stochastic manner [36]. These features could be the cause of the dramatic enhancement of the reprogramming efficiency from PMNCs in the T-cell-stimulating medium.

EBNA1 was also reported to have a correlation with the *TP53* signaling. *TP53* is an important molecule that regulates the cell cycle. EBNA1 interacts with the N-terminal domain of a ubiquitin-specific protease, USP7 [37]. USP7 can also bind *TP53* through its N-terminal domain, which results in the stabilization of *TP53* [38]. Hence, both EBNA1 and *TP53* interact with USP7, and EBNA1 is thought to interfere with the stabilization of *TP53* by blocking their interaction. Therefore, transient high expression of EBNA1 and a shRNA for *TP53* encoded by Y4 would synergistically suppress the endogenous *TP53* and enhance the reprogramming process.

When 3×10^6 PMNCs were used for electroporation, one-tenth of them generated 130.8 colonies in the T-cell medium (0.04%) and one-third of them gave 5.4 colonies in the non-T-cell medium (0.0005%) on average. During the reprogramming process under the T-cell condition, however, one transduced T cell would produce dozens of daughter cells, which would inherit episomal vectors. In support of this, identical TRB rearrangements were observed in different iPS clones established from the same dish, suggesting that the cells were derived from one parental T cell (Supporting Information Fig. S8). Only a portion of these amplified daughter cells would enter the reprogramming process, attach to the culture dish, and form iPS colonies. Hence, the actual efficiency was likely much lower than the estimated efficiency. Conversely, we replaced the culture medium on day 4, in which most cells were floating. The supernatant still had the potential to induce iPSC colonies when they were seeded onto new feeder cells (data not shown). Therefore, our culture protocol likely led to the loss of many cells that had acquired some initiation into the reprogramming process. The reported iPSC induction efficiency by retro/lentivirus vectors is around 0.002% [18, 39] and 0.02% [8] from normal and mobilized peripheral blood, respectively. The nonintegration method using episomal vector C1 would be less efficient (0.001%) than those [12]. Mack et al. purified and expanded $CD34^+$ cells from PMNCs and carried out transduction with episomal vectors, which were similar to T1, but used L-MYC instead of C-MYC [17]. They estimated that the reprogramming efficiency was 0.03% on average and obtained approximately five iPSC colonies per 1 ml of blood. With similar approach, our mixture Y4+EBNA1 showed the reprogramming efficiency around 0.06%, which was twofold higher than that of the previous report. To the best of our knowledge, this study describes the most efficient simple method to generate iPSCs from peripheral blood by a nonviral vector.

Conclusion

In this study, we developed a method that can be used to generate iPSCs from cord blood and PMNCs. The efficiency from PMNCs was up to 0.1% at the maximum. This means that only a few milliliters of peripheral blood is sufficient for the induction of iPSCs. Frozen cells can also be applied for the induction. Thus, our report provides a practical and efficient way to generate patient-specific iPSCs. This will also be valuable for the generation of clinical-grade iPSCs for future therapeutic applications.

Acknowledgments

We thank T. Aoi, K. Takahashi, M. Nakagawa, and Y. Yoshida for scientific discussion; M. Narita, T. Ichisaka, and M. Ohuchi for technical assistance; R. Kato, E. Nishikawa, S. Takeshima, and Y. Ohtsu for administrative assistance; and Drs. H. Niwa (Riken) and J. Miyazaki (Osaka Univ.) for the CAG promoter. This study was supported in part by a grant from the Program for Promotion of Fundamental Studies in Health Sciences of National Institute of Biomedical Innovation, a grant from the Leading Project of Ministry of Education, Culture, Sports, Science and Technology (MEXT), a grant from Funding Program for World-Leading Innovative Research and Development on Science and Technology (FIRST Program) of Japan Society for the Promotion of Science, Grants-in-Aid for Scientific Research of Japan Society for the Promotion of Science and MEXT (to S.Y.), and Grants-in-Aid for Scientific Research for Young Scientists B (to K.O.).

Disclosure of Potential Conflicts of Interest

K.O. and S.Y. are filing a patent application based on the results reported in this paper. S.Y. is a member without salary of the scientific advisory boards of iPierian, iPS Academia Japan, Megakaryon Corporation, and Retina Institute Japan.

References

1 Takahashi K, Yamanaka S. Induction of pluripotent stem cells from mouse embryonic and adult fibroblast cultures by defined factors. Cell 2006;126:663–676.

2 Takahashi K, Tanabe K, Ohnuki M et al. Induction of pluripotent stem cells from adult human fibroblasts by defined factors. Cell 2007; 131:861–872.

3 Yu J, Vodyanik MA, Smuga-Otto K et al. Induced pluripotent stem cell lines derived from human somatic cells. Science 2007;318: 1917–1920.

4 Hotta A, Cheung AY, Farra N et al. Isolation of human iPS cells using EOS lentiviral vectors to select for pluripotency. Nat Methods 2009;6:370–376.

5 Park IH, Arora N, Huo H et al. Disease-specific induced pluripotent stem cells. Cell 2008;134:877–886.

6 Sun N, Panetta NJ, Gupta DM et al. Feeder-free derivation of induced pluripotent stem cells from adult human adipose stem cells. Proc Natl Acad Sci USA 2009;106:15720–15725.
7 Aasen T, Raya A, Barrero MJ et al. Efficient and rapid generation of induced pluripotent stem cells from human keratinocytes. Nat Biotechnol 2008;26:1276–1284.
8 Loh YH, Agarwal S, Park IH et al. Generation of induced pluripotent stem cells from human blood. Blood 2009;113:5476–5479.
9 Seki T, Yuasa S, Oda M et al. Generation of induced pluripotent stem cells from human terminally differentiated circulating T cells. Cell Stem Cell 2010;7:11–14.
10 Yu J, Hu K, Smuga-Otto K et al. Human induced pluripotent stem cells free of vector and transgene sequences. Science 2009;324: 797–801.
11 Yu J, Chau KF, Vodyanik MA et al. Efficient feeder-free episomal reprogramming with small molecules. PLoS One 2011;6:e17557.
12 Chou BK, Mali P, Huang X et al. Efficient human iPS cell derivation by a non-integrating plasmid from blood cells with unique epigenetic and gene expression signatures. Cell Res 2011;21:518–529.
13 Okita K, Matsumura Y, Sato Y et al. A more efficient method to generate integration-free human iPS cells. Nat Methods 2011;8:409–412.
14 McMahon AP, Bradley A. The Wnt-1 (int-1) proto-oncogene is required for development of a large region of the mouse brain. Cell 1990;62:1073–1085.
15 Fujioka T, Yasuchika K, Nakamura Y et al. A simple and efficient cryopreservation method for primate embryonic stem cells. Int J Dev Biol 2004;48:1149–1154.
16 Niwa H, Yamamura K, Miyazaki J. Efficient selection for high-expression transfectants with a novel eukaryotic vector. Gene 1991; 108:193–199.
17 Mack AA, Kroboth S, Rajesh D et al. Generation of induced pluripotent stem cells from CD34+ cells across blood drawn from multiple donors with non-integrating episomal vectors. PLoS One 2011;6: e27956.
18 Loh YH, Hartung O, Li H et al. Reprogramming of T cells from human peripheral blood. Cell Stem Cell 2010;7:15–19.
19 DePristo MA, Banks E, Poplin R et al. A framework for variation discovery and genotyping using next-generation DNA sequencing data. Nat Genet 2011;43:491–498.
20 Ye Z, Zhan H, Mali P et al. Human-induced pluripotent stem cells from blood cells of healthy donors and patients with acquired blood disorders. Blood 2009;114:5473–5480.
21 Ohgushi M, Matsumura M, Eiraku M et al. Molecular pathway and cell state responsible for dissociation-induced apoptosis in human pluripotent stem cells. Cell Stem Cell 2010;7:225–239.
22 Park IH, Zhao R, West JA et al. Reprogramming of human somatic cells to pluripotency with defined factors. Nature 2008;451:141–146.
23 Tsubooka N, Ichisaka T, Okita K et al. Roles of Sall4 in the generation of pluripotent stem cells from blastocysts and fibroblasts. Genes Cells 2009;14:683–694.
24 Feng B, Jiang J, Kraus P et al. Reprogramming of fibroblasts into induced pluripotent stem cells with orphan nuclear receptor Esrrb. Nat Cell Biol 2009;11:197–203.
25 Han J, Yuan P, Yang H et al. Tbx3 improves the germ-line competency of induced pluripotent stem cells. Nature 2010;463:1096–1100.
26 Maekawa M, Yamaguchi K, Nakamura T et al. Direct reprogramming of somatic cells is promoted by maternal transcription factor Glis1. Nature 2011;474:225–229.
27 Marson A, Foreman R, Chevalier B et al. Wnt signaling promotes reprogramming of somatic cells to pluripotency. Cell Stem Cell 2008; 3:132–135.
28 Edel MJ, Menchon C, Menendez S et al. Rem2 GTPase maintains survival of human embryonic stem cells as well as enhancing reprogramming by regulating p53 and cyclin D1. Genes Dev 2010;24:561–573.
29 Zhao Y, Yin X, Qin H et al. Two supporting factors greatly improve the efficiency of human iPSC generation. Cell Stem Cell 2008;3: 475–479.
30 Mali P, Ye Z, Hommond HH et al. Improved efficiency and pace of generating induced pluripotent stem cells from human adult and fetal fibroblasts. Stem Cells 2008;26:1998–2005.
31 Subramanyam D, Lamouille S, Judson RL et al. Multiple targets of miR-302 and miR-372 promote reprogramming of human fibroblasts to induced pluripotent stem cells. Nat Biotechnol 2011;29:443–448.
32 Peterson C, Legerski R. High-frequency transformation of human repair-deficient cell lines by an Epstein-Barr virus-based cDNA expression vector. Gene 1991;107:279–284.
33 Gore A, Li Z, Fung HL et al. Somatic coding mutations in human induced pluripotent stem cells. Nature 2011;471:63–67.
34 Serwold T, Hochedlinger K, Inlay MA et al. Early TCR expression and aberrant T cell development in mice with endogenous prerearranged T cell receptor genes. J Immunol 2007;179:928–938.
35 Trickett A, Kwan YL. T cell stimulation and expansion using anti-CD3/CD28 beads. J Immunol Methods 2003;275:251–255.
36 Hanna J, Saha K, Pando B et al. Direct cell reprogramming is a stochastic process amenable to acceleration. Nature 2009;462:595–601.
37 Saridakis V, Sheng Y, Sarkari F et al. Structure of the p53 binding domain of HAUSP/USP7 bound to Epstein-Barr nuclear antigen 1 implications for EBV-mediated immortalization. Mol Cell 2005;18: 25–36.
38 Li M, Chen D, Shiloh A et al. Deubiquitination of p53 by HAUSP is an important pathway for p53 stabilization. Nature 2002;416:648–653.
39 Staerk J, Dawlaty MM, Gao Q et al. Reprogramming of human peripheral blood cells to induced pluripotent stem cells. Cell Stem Cell 2010;7:20–24.

See www.StemCells.com for supporting information available online.

Molecular and Cellular Biology

Noncanonical NOTCH Signaling Limits Self-Renewal of Human Epithelial and Induced Pluripotent Stem Cells through ROCK Activation

Takashi Yugawa, Koichiro Nishino, Shin-ichi Ohno, Tomomi Nakahara, Masatoshi Fujita, Naoki Goshima, Akihiro Umezawa and Tohru Kiyono

Mol. Cell. Biol. **2013, 33(22):4434. DOI: 10.1128/MCB.00577-13.**
Published Ahead of Print 9 September 2013.

MCB
Journals.ASM.org

Noncanonical NOTCH Signaling Limits Self-Renewal of Human Epithelial and Induced Pluripotent Stem Cells through ROCK Activation

Takashi Yugawa,[a] Koichiro Nishino,[b] Shin-ichi Ohno,[a] Tomomi Nakahara,[a] Masatoshi Fujita,[c] Naoki Goshima,[d] Akihiro Umezawa,[e] Tohru Kiyono[a]

Division of Virology, National Cancer Center Research Institute, Tokyo, Japan[a]; Laboratory of Veterinary Biochemistry and Molecular Biology, Faculty of Agriculture, University of Miyazaki, Miyazaki, Japan[b]; Department of Cellular Biochemistry, Graduate School of Pharmaceutical Sciences, Kyushu University, Fukuoka, Japan[c]; Molecular Profiling Research Center for Drug Discovery, National Institute of Advanced Industrial Science and Technology, Tokyo, Japan[d]; Department of Reproductive Biology, National Center for Child Health and Development, Tokyo, Japan[e]

NOTCH plays essential roles in cell fate specification during embryonic development and in adult tissue maintenance. In keratinocytes, it is a key inducer of differentiation. ROCK, an effector of the small GTPase Rho, is also implicated in keratinocyte differentiation, and its inhibition efficiently potentiates immortalization of human keratinocytes and greatly improves survival of dissociated human pluripotent stem cells. However, the molecular basis for ROCK activation is not fully established in these contexts. Here we provide evidence that intracellular forms of NOTCH1 trigger the immediate activation of ROCK1 independent of its transcriptional activity, promoting differentiation and resulting in decreased clonogenicity of normal human keratinocytes. Knockdown of NOTCH1 abrogated ROCK1 activation and conferred sustained clonogenicity upon differentiation stimuli. Treatment with a ROCK inhibitor, Y-27632, or ROCK1 silencing substantially rescued the growth defect induced by activated NOTCH1. Furthermore, we revealed that impaired self-renewal of human induced pluripotent stem cells upon dissociation is, at least in part, attributable to NOTCH-dependent ROCK activation. Thus, the present study unveils a novel NOTCH-ROCK pathway critical for cellular differentiation and loss of self-renewal capacity in a subset of immature cells.

Notch is an evolutionarily conserved cell surface receptor that plays essential roles in cell fate decisions as well as maintenance of self-renewing tissue organization (1–3). Notch proteins are expressed in most adult tissues, and the biological consequence of Notch activation is critically dependent on the cell type and the cellular context (4–7). In keratinocytes, Notch1 has been shown to be a key inducer of differentiation (8–11). Keratinocyte-specific conditional deletion of the *Notch1* gene results in epidermal hyperproliferation and tumor formation in mice, thus indicating a tumor-suppressive role of Notch1 in mammalian postnatal epidermis (12). The Notch receptor is generally activated by interaction with its ligands displayed on the neighboring cell surface. Cell-cell contact is a strong inducer of keratinocyte differentiation in culture, where Notch1 acts as a critical determinant in the transition from proliferation to differentiation (13, 14). Due to *cis* inhibition of Notch by its ligand when these are expressed on the same cell surface (15, 16), the relative increase in expression levels of the Notch receptor over its ligand is also shown to be a pivotal cue to activate Notch signaling and generate distinct cell fates among neighboring cells (17). We previously demonstrated that p53 and TAp63 transactivate *Notch1* gene expression and induce keratinocyte differentiation, while ΔNp63 is a transcriptional repressor of the *Notch1* gene and inhibits keratinocyte differentiation (14, 18). p63, especially ΔNp63α, is a master regulator of development and maintenance of stratified epithelia (19, 20). ΔNp63α expresses predominantly in the basal proliferating compartment, where Notch1 signaling is suppressed (21). In suprabasal layers, downregulation of ΔNp63α by miR-203 or another factor(s) (22–24) evokes activation of Notch1 signaling, which in turn further downmodulates ΔNp63α expression so as to induce differentiation (9, 21). The Notch1 precursor (~300 kDa) is processed by furin protease in the Golgi apparatus and transported to the cell surface as a mature heterodimeric complex (~120/~180 kDa) that is held by Ca^{2+}-dependent noncovalent interaction (25). Ligand binding dissociates the Notch1 extracellular domain (~180 kDa) by *trans* endocytosis. The residual transmembrane domain (~120 kDa) is sequentially cleaved by tumor necrosis factor alpha-converting enzyme/metalloprotease (TACE) and γ-secretase, resulting in release of the Notch1 intracellular domain (~110 kDa) into the cytosol (3). EDTA is reported to activate Notch signaling through disruption of the heterodimeric complex of Notch1 (25) and thus used as a tool to study Notch1 signaling (26–28). In canonical Notch1 signaling, the liberated Notch1 intracellular domain (~110 kDa) translocates into the nucleus to activate Notch-responsive genes, such as Hes1, by making a complex with CSL family members {CBF1 and RBP-Jκ in mammals, Suppressor of hairless [Su(H)] in *Drosophila*, and Lag1 in *Caenorhabditis elegans*} and its transcriptional coactivator Mastermind (MAM). Besides this canonical pathway, accumulating evidence suggests noncanonical cytoplasmic Notch functions (29–31).

Received 11 May 2013 Returned for modification 5 June 2013
Accepted 20 August 2013
Published ahead of print 9 September 2013
Address correspondence to Tohru Kiyono, tkiyono@ncc.go.jp.
Supplemental material for this article may be found at http://dx.doi.org/10.1128/MCB.00577-13.

doi:10.1128/MCB.00577-13

Rho-associated coiled-coil protein kinases (ROCKs) (also known as Rho kinases [ROKs]) are effectors of the small GTPase Rho and belong to a family of protein serine/threonine kinases (32–34). Activated ROCK proteins regulate actomyosin cytoskeletal dynamics and contractility through phosphorylation of multiple downstream targets, such as myosin phosphatase (MYPT1), to drive cell motility. In keratinocytes, ROCK proteins play a role in differentiation (35, 36), and their selective inhibitor, Y-27632, completely inhibits differentiation as well as stratification of keratinocytes in organotypic raft culture (37). Y-27632 also enables efficient immortalization of not only human primary keratinocytes but also several other primary human epithelial cells in the presence of fibroblast feeders (37, 38), although molecular details supporting immortalization remain elusive.

In addition, Y-27632 has been shown to increase the survival rate and cloning efficiency of human embryonic stem cells (hESCs) dissociated with EDTA (39) through blocking the Rho-ROCK-myosin light chain signaling cascade (40, 41). However, the precise mechanisms by which EDTA activates ROCK have not been elucidated (41, 42).

These results let us hypothesize a possible link between NOTCH1 and ROCK activation. Here we show a novel function of NOTCH1 as a critical upstream regulator of ROCK1 and its relevance to loss of self-renewal capacity in human keratinocytes as well as human induced pluripotent stem (hiPS) cells.

MATERIALS AND METHODS

Cell culture. Normal human cervical keratinocytes (HCKs) were obtained with written consent from a patient who underwent abdominal surgery for a gynecological disease other than cervical cancer and were retrovirally transduced with the catalytic subunit of human telomerase reverse transcriptase (hTERT) for immortalization (HCK1Ts) (14). HCK1Ts were cultured in serum-free keratinocyte-SF medium supplemented with 5 ng/ml epidermal growth factor (EGF) and 50 μg/ml of bovine pituitary extract (Invitrogen, Life Technologies, Saint Aubin, France). Primary human dermal keratinocytes (HDKs) were purchased from Cell Applications Inc. (San Diego, CA). Primary human foreskin keratinocytes (HFKs) were obtained from Denise A. Galloway (Fred Hutchinson Cancer Research Center, Seattle, WA). HDKs and HFKs were cultured in serum-free keratinocyte-SF medium supplemented with 5 ng/ml EGF and 50 μg/ml of bovine pituitary extract (Invitrogen, Life Technologies). Human endometrium cells were collected by scraping tissues from surgical specimens, with signed informed consent and with ethical approval of the Institutional Review Board of the National Institute for Child Health and Development, Japan. All experiments involving human cells and tissues were performed in line with Tenets of the Declaration of Helsinki. Human iPS cell lines, MRC-hiPSCs and UtE-hiPSCs, were established from MRC-5 fetal lung fibroblasts (43) and UtE1104 endometrium-derived cells (44), respectively, via procedures described by Takahashi et al. (45) with slight modification (46, 47). Human iPS cells were maintained in iPSellon medium (Cardio Incorporated, Osaka, Japan) supplemented with 10 ng/ml recombinant human basic fibroblast growth factor (bFGF) (Wako Pure Chemical Industries, Ltd., Osaka, Japan) in the presence of irradiated mouse embryonic fibroblast (MEF) feeders.

Retroviral vector construction and transduction. Retroviral vector plasmids were constructed using the Gateway system according to the manufacturer's instructions (Invitrogen). Segments of the intracellular domain of human NOTCH1 (ICN1), a truncated form of MAML1 corresponding to amino acids 13 to 74 fused to N-terminal hemagglutinin (HA) tag (MAML61-3HA), and c-MYC were cloned and recombined into retroviral expression vectors to generate pCLXSN-ICN1 (14), pCLXSN-MAML61-3HA (48, 49), and pCMSCVpuro-c-MYC (50). Human ROCK1, ROCK1ΔC241, ROCK1-D1113A, ROCK1-K105A, ICN1-ERT, ICN2-ERT2, RhoA, and enhanced green fluorescent protein (EGFP) were cloned into a lentiviral vector, CSII-TRE-Tight-RfA, in which the elongation factor promoter in CSII-EF-RfA (a gift from Hiroyuki Miyoshi, RIKEN, BioResource Center) was replaced with the tetracycline-responsive promoter from pTRE-Tight (Clontech, Mountain View, CA). The Notch1 short hairpin RNA (shRNA) vectors were described previously (14, 18). To generate ROCK1- or ROCK2-specific shRNA expression vectors pCL-SI-MSCVpuro-ROCK1Ri-1,-2,-3 and pCL-SI-MSCVpuro-ROCK2Ri-1,-2,-3, the following sequences were chosen as the targeted sites: 5′-GTACTTGTATGAAGATGA-3′ (51), 5′-GGTATATGCTATGAAGCTT-3′, and 5′-GCGAAATGGTGTAGAAGAA-3′ for ROCK1 and 5′-GAAACTAATAGGACACTAAC-3′ (52), 5′-GGTTTATGCTATGAAGCTT-3′, and 5′-GGATAAACATGGACATCTA-3′ for ROCK2. The retroviral vector and packaging constructs pCL-GagPol and pEF6/env (10A1) or the lentiviral vector and packaging constructs pCAG-HIVgp and pCMV-VSV-G-RSV-Rev were cotransfected into 293FT cells (Invitrogen) using TransIT-293 (Mirus Co., Madison, WI) according to the manufacturer's instructions, and the culture fluid was harvested at 60 to 72 h posttransfection. Titers of the recombinant viruses were determined by drug resistance with HeLa cells or a real-time PCR method (TaKaRa, Otsu, Japan) to detect the viral RNA genome, yielding titers equivalent to greater than 1×10^6 CFU/ml. Following addition of the recombinant viral fluid to cells in the presence of 4 μg/ml Polybrene, infected cells were selected in the presence of 0.5 μg/ml puromycin or 50 μg/ml G418, and promptly after drug selection, pooled cell populations were used for most subsequent experiments.

Tet-On keratinocytes. HCK1T cells were stably transduced with Tet-On ADV and tTS expression vectors, encoding the rtTA-Advanced transactivator and transcriptional silencer, respectively (Clontech). The resultant HCK1T Tet-On cells were then introduced with CSII-TRE-Tight-ROCK1, ROCK1ΔC241, ROCK1-D1113A, ROCK1-K105A, ICN1-ERT, ICN2-ERT2, RhoA (constitutive active and dominant negative forms), and EGFP by retroviral gene transfer. Induction of these transgenes was routinely achieved by treatment with 1 μg/ml doxycycline (DOX) for 72 h.

Inhibitors. The following pharmacological inhibitors were used: cycloheximide (CHX) (239764; Calbiochem, Darmstadt, Germany), z-VAD-fmk (caspase inhibitor IV) (219007; Calbiochem), γ-secretase inhibitor IX (DAPT) (565784; Calbiochem), Y-27632 (08945-84; Nacalai Tesque, Kyoto, Japan), C3 ADP-ribosyltransferase (Rho inhibitor) (CT04; Cytoskeleton, Inc., Denver, CO), and blebbistatin (sc-203532; Santa Cruz Biotechnology, Santa Cruz, CA). Cells were pretreated with inhibitors for 2.5 h. For DAPT, in addition to pretreatment, cells were incubated with this inhibitor during and after exposure to EDTA or differentiation stimuli for up to 48 h.

Induction of keratinocyte differentiation. At 48 h after plating, HCK1T cells were treated with 2.5 mM EDTA in phosphate-buffered saline without Ca^{2+} and Mg^{2+} [PBS(−)] for 10 min or exposed to 0.7% and 5% bovine serum albumin (BSA) or 10% serum-containing medium in the presence of 10 μg/ml of bovine pituitary extract. To induce ligand-dependent NOTCH activation, HCK1T cells were harvested in subconfluent and 7-day-postconfluent states. HCK1T cells were also introduced with ICN1 by retroviral gene transfer to induce differentiation.

Dissociation of human iPS cells. First, hiPSC colonies were treated with collagenase IV solution at 37°C for 10 min. The detached hiPSC clumps were recovered, incubated with 0.005% trypsin–2.5 mM EDTA solution at 37°C for 5 min, and dissociated into single cells by pipetting. The dissociated cells were counted with Vi-CELL (Beckman Coulter, Brea, CA) and seeded onto MEF feeders.

Immunoblotting. Whole-cell protein extracts were used for analysis, and immunoblotting was conducted as described previously (14). Primary antibodies against Notch1 (sc-6014; Santa Cruz Biotechnology), activated Notch1 (cleaved Notch1 Val1744 2421; Cell Signaling Technology, Danvers, MA), Notch2 (clone C651.6DbHN; Developmental Studies Hybridoma Bank, University of Iowa), Hes1 (Toray Industries, Inc., To-

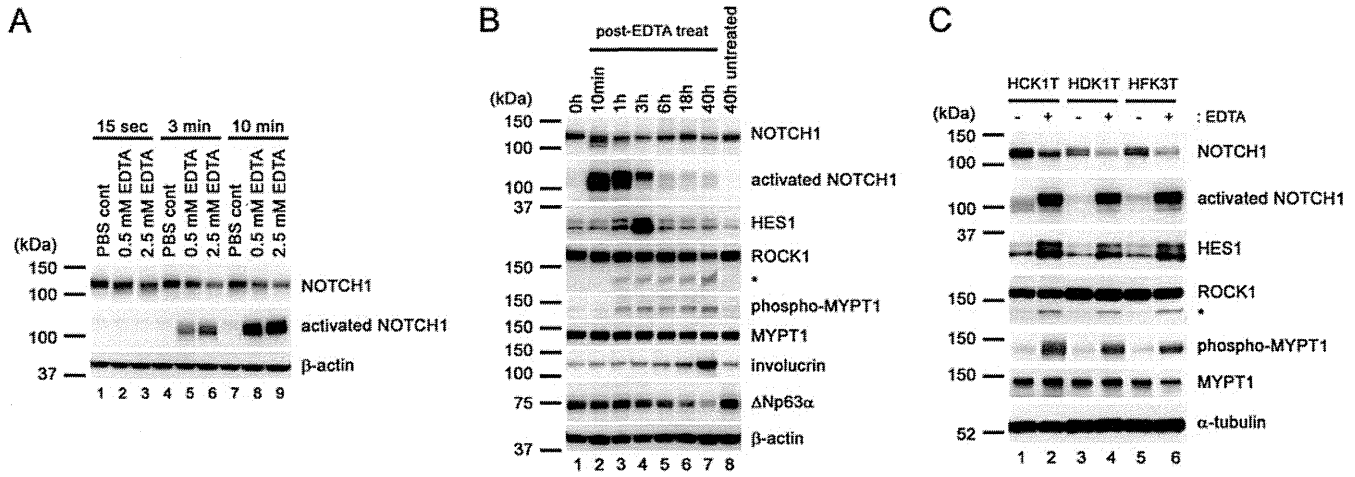

FIG 1 Immediate activation of ROCK1 following release of the NOTCH1 intracellular fragment in normal human keratinocytes. (A) HCK1T cells were either left untreated (PBS cont) or treated with 0.5 or 2.5 mM EDTA in PBS(−) for indicated time points. Cell lysates were prepared and analyzed by immunoblotting with the indicated antibodies. (B) HCK1T cells were either left untreated or treated with 2.5 mM EDTA in PBS(−) for 10 min at 37°C. After washing twice with PBS(−), cells were incubated with keratinocyte-SF medium. Cell lysates were prepared at the indicated time points after EDTA treatment. Extracts were analyzed by immunoblotting with the indicated antibodies. The band corresponding to the furin-processed transmembrane domain of NOTCH1 with a molecular mass of 120 kDa is shown as NOTCH1 here. An asterisk indicates a smaller fragment of ROCK1 protein with a molecular mass of ~130 kDa. (C) Keratinocytes from cervix (HCK1T), dermis (HDK1T), and foreskin (HFK1T) were either left untreated or treated with 2.5 mM EDTA for 10 min. After washing twice with PBS(−), cells were incubated with keratinocyte-SF medium for 3 h. Extracts were analyzed by immunoblotting with the indicated antibodies.

kyo, Japan), Hey1 (sc-16424; Santa Cruz Biotechnology), involucrin (clone SY5; Sigma, Saint-Quentin Fallavier, France), loricrin (AF 62; Covance, Princeton, NJ), Rock1 (sc-5560; Santa Cruz Biotechnology), phospho-MYPT1 (07-251; Merck-Millipore, Billerica, MA), MYPT1 (07-672; Merck-Millipore), Rock2 (sc-5561; Santa Cruz Biotechnology), p63 (clone 4A4; Santa Cruz Biotechnology), caspase-3 (9662; Cell Signaling Technology), poly(ADP-ribose) polymerase (PARP) (9542; Cell Signaling Technology), OCT3/4 (sc-5279; Santa Cruz Biotechnology), HA tag

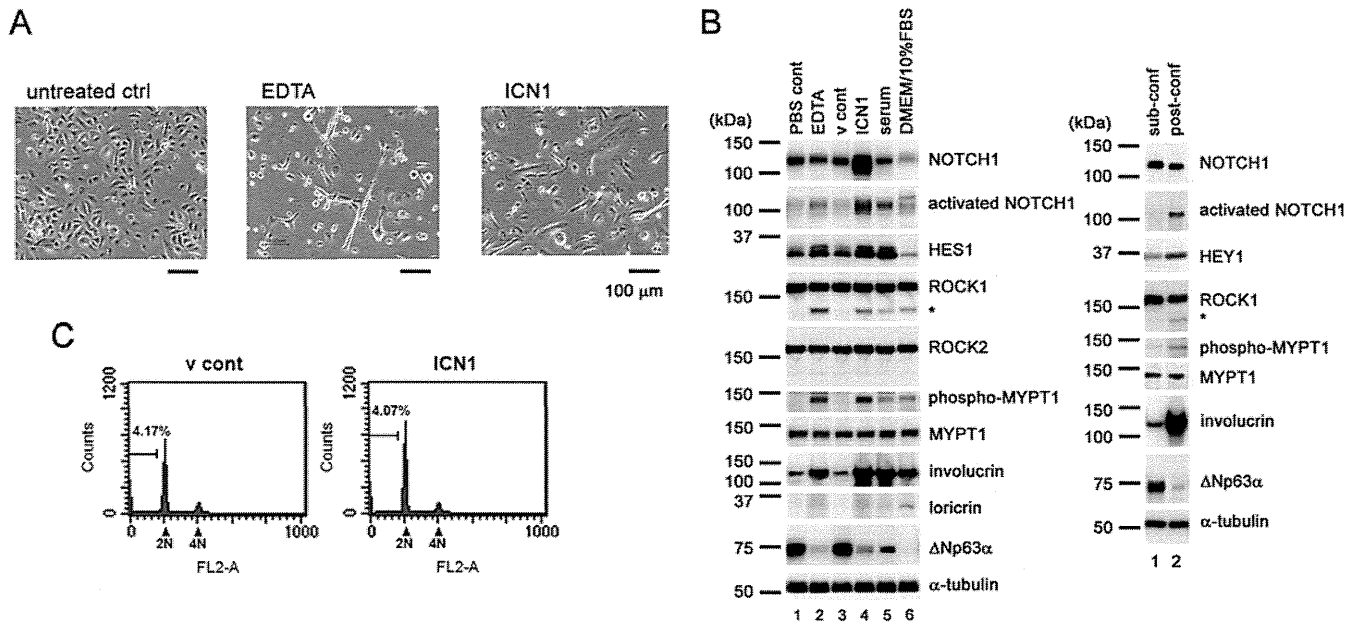

FIG 2 Expression of the NOTCH1 intracellular domain, serum exposure, and cell-cell contact cause ROCK activation and cellular differentiation in normal keratinocytes. (A) HCK1T cells were either left untreated or treated with 2.5 mM EDTA and incubated with keratinocyte-SF medium after treatment. HCK1T cells were transduced with the constitutively active form of NOTCH1 (ICN1). Typical areas were photographed at 3 days posttreatment or posttransduction. Scale bars represent 100 μm. (B) HCK1T cells were either left untreated or treated with 2.5 mM EDTA and incubated with keratinocyte-SF medium after treatment. HCK1T cells were transduced with the constitutively active form of NOTCH1 (ICN1) or control (v cont). HCK1T cells were exposed to serum-containing keratinocyte-SF medium (serum) or Dulbecco modified Eagle medium with 10% fetal bovine serum (DMEM–10% FBS). Cell lysates were harvested at 3 days posttreatment or posttransduction. HCK1T cells were also harvested in subconfluent and 7-day-postconfluent states. Extracts were analyzed by immunoblotting with the indicated antibodies. (C) HCK1T cells were transduced with the constitutively active form of NOTCH1 (ICN1) or control (v cont). At 3 days posttransduction, cells were collected and DNA content was analyzed by flow cytometry. The percentage of apoptotic cells displaying a sub-G_1 DNA content is shown between markers.

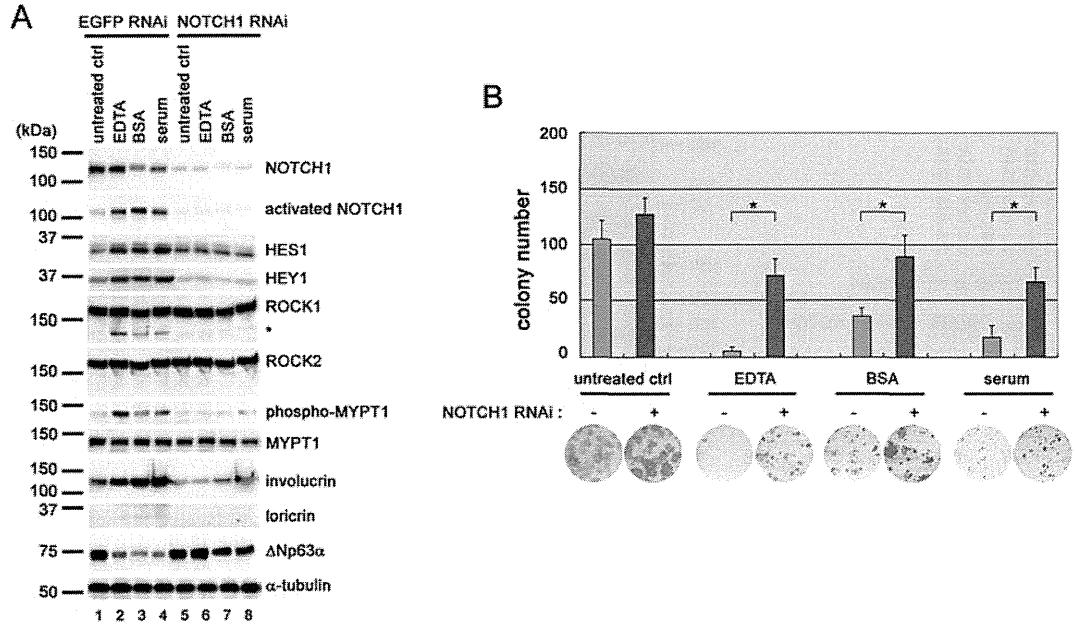

FIG 3 Knockdown of NOTCH1 abrogates the production of the smaller ROCK1 and MYPT1 phosphorylation with restoration of clonogenic growth potential in normal keratinocytes exposed to EDTA, BSA, or serum. (A) HCK1T cells stably expressing NOTCH1 shRNA (NOTCH1 RNAi) or control shRNA (EGFP RNAi) were treated with 2.5 mM EDTA, 5% bovine serum albumin, or 10% serum or left untreated. Cells were harvested at 3 days posttreatment, and cell extracts were subjected to immunoblotting analysis with the indicated antibodies. (B) Aliquots of 500 HCK1T cells stably expressing NOTCH1 shRNA (NOTCH1 RNAi) or control shRNA (EGFP RNAi) were seeded on 35-mm dishes under sparse conditions. Then cells were treated similarly to those for panel A. After being cultivated for 2 weeks, the cells were stained with Giemsa's dye, and colonies were counted. The photographs are of representative dishes, and the graph represents means ± SDs. *, $P < 0.05$ according to Student's *t* tests.

(ab72479; Abcam, Paris, France), β-actin (sc-1616; Santa Cruz Biotechnology), α-tubulin (2144; Cell Signaling Technology), and GAPDH (glyceraldehyde-3-phosphate dehydrogenase) (AM4300; Ambion, Inc., Austin, TX) were used as probes. Horseradish peroxidase-conjugated anti-mouse and anti-rabbit (Jackson ImmunoResearch Laboratories, West Grove, PA) and anti-goat (sc-2033; Santa Cruz Biotechnology) immunoglobulins were used as the secondary antibodies. The LAS3000 charge-coupled device (CCD) imaging system (Fujifilm Co. Ltd., Tokyo, Japan) was employed for detection of proteins visualized by Lumi-light Plus Western blotting substrate (Roche, Basel, Switzerland). The exposure time was adjusted to keep the signals within a linear and nonsaturated range, and the band signal intensities were quantified by densitometry using imaging software (Fujifilm Multi-Gauge) after normalization to that of internal controls, such as β-actin, α-tubulin, or GAPDH.

Fluorescence-activated cell sorting analysis. Cells were treated with a CycleTEST Plus DNA reagent kit (Becton Dickinson, Franklin Lakes, NJ) for propidium iodide staining and then analyzed with a Becton Dickinson FACSCalibur instrument.

Clonogenic assay. Aliquots of 500 cells were seeded on 35-mm dishes under sparse conditions. After cultivation for 2 weeks, the cells were stained with Giemsa's dye, and the colonies were counted.

Statistical analysis. Statistical analysis was carried out using Microsoft Excel software. Unless stated otherwise, all data are presented as means ± standard deviations (SD) from at least three independent experiments; error bars represent SD in all figures. Intergroup comparisons were performed by the two-tailed Student's *t* test. A *P* value of <0.05 was considered to be statistically significant.

RESULTS

Immediate activation of ROCK following expression of the NOTCH intracellular form. Previous work has shown stabilization of the noncovalent interaction between a ligand-binding extracellular domain and a transmembrane signaling subunit of NOTCH by millimolar Ca^{2+} and transient activation of this heterodimeric NOTCH receptor by EDTA-mediated shedding of its extracellular domain, independent of cell-cell contact or binding of a ligand displayed on the surface of a neighboring cell (25). In line with this notion, somatic activating mutations of NOTCH1 within the heterodimerization domain are frequently found in human T cell acute lymphoblastic leukemia and are thought to increase the production of the intracellular form of NOTCH1 (53). To ascertain whether calcium depletion could induce activation of NOTCH1, normal human keratinocytes, which were maintained with serum-free, low-calcium medium, were subjected to EDTA treatment. We found that this chelator treatment elicited immediate and robust expression of the cleaved intracellular form of NOTCH1 in a time- and dose-dependent manner (Fig. 1A). Time course experiments revealed that this intracellular NOTCH1 arose transiently and that thereafter activation of the NOTCH target gene was induced, as well as upregulation of a differentiation marker and downregulation of a keratinocyte stemness marker, ΔNp63α, in agreement with its proposed role in keratinocyte differentiation (Fig. 1B) (8, 9, 11). We also noted that the EDTA-treated cells underwent a drastic morphological change (Fig. 2A) with increased motility (see Movie S1 in the supplemental material), which was also seen in cells transduced with the NOTCH1 intracellular domain (ICN1) in much the same fashion (Fig. 2A). We have previously shown that these morphologically altered cells are differentiating cells strongly expressing K10 and involucrin (14).

ROCK inhibition with Y-27632 has been reported to inhibit differentiation and increase the proliferative capacity of primary human keratinocytes in culture, pointing to a role for ROCK

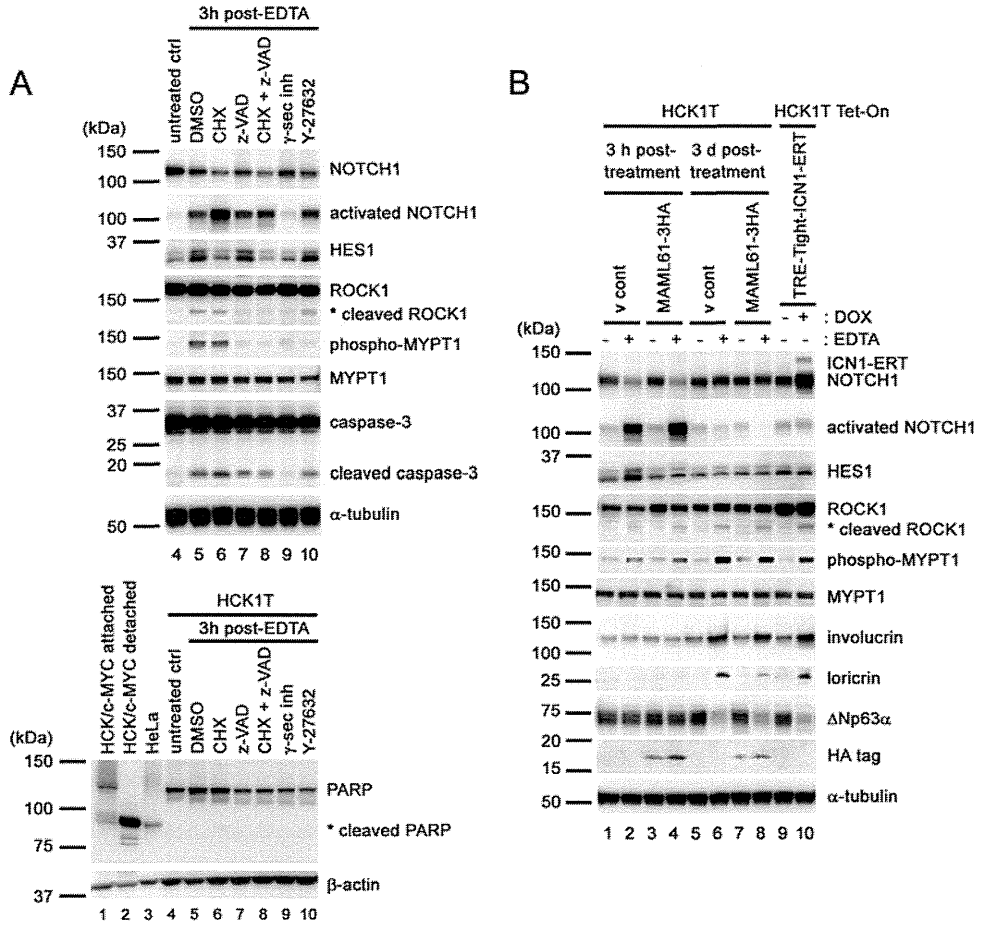

FIG 4 ROCK1 activation is independent of NOTCH1 transcriptional activity. (A) HCK1T cells, pretreated where indicated with 10 μg/ml cycloheximide (CHX) for 2.5 h, 20 μM z-VAD-fmk for 2.5 h, 10 μM γ-secretase inhibitor (DAPT) for 2.5 h, or 10 μM Y-27632 for 2.5 h, were either left untreated or treated with 2.5 mM EDTA for 10 min and incubated with keratinocyte-SF medium for 3 h. Whole-cell extracts were subjected to immunoblotting analysis with the indicated antibodies. As a positive control for PARP cleavage, cell extracts from detached HCKs after c-MYC transduction were used. (B) HCK1T cells were stably transduced with dominant negative MAML1 (MAML61-3HA) or vector control (v cont). Cells were exposed to 2.5 mM EDTA (+) or left untreated (−), and cell lysates were prepared at 3 h and 72 h posttreatment. HCK1T Tet-On cells were then introduced with the TRE-Tight-ICN1-ERT tetracycline-inducible gene cassette. HCK1T Tet-On-ICN1-ERT cells were either left untreated (−) or treated (+) with 1 μg/ml doxycycline (DOX) for 72 h.

in keratinocyte differentiation (35, 37). These observations prompted us to determine whether NOTCH activation by EDTA treatment during passage could induce differentiation or a decrease in proliferative potential, possibly through ROCK activation. As shown in Fig. 1B, immediately after production of the NOTCH1 intracellular form, additional ROCK1 polypeptides of smaller size emerged. The ROCK1 fragment with a relative molecular weight of ~130,000 was reminiscent of that observed in cells undergoing apoptosis, which has been identified as a caspase-3-cleaved, constitutively activated form (54, 55). Indeed, MYPT1, a downstream molecule of ROCK, was phosphorylated concomitantly with the appearance of the smaller ROCK1 proteins, indicating increased ROCK1 activity in cells with active NOTCH1 signaling.

In keratinocytes, NOTCH1 has been shown to be activated in response to differentiation stimuli such as suspension in methylcellulose, confluence-triggered cell-cell contact, and serum exposure, as well as with genotoxic stress (13, 14, 18, 49, 56). Therefore, we examined whether differentiation stimuli or expression of ICN1 could cause ROCK activation. The additional smaller proteins of ROCK1, but not ROCK2, and phosphorylation of MYPT1 were observed in response to serum exposure (Fig. 2B, left panel). Since albumin is the major protein in serum, to which approximately half of extracellular calcium is bound, we further tested the possibility that albumin exerts a differentiation-inducing effect through a mechanism similar to that for EDTA. As expected, albumin exposure also induced activation of NOTCH1, production of the smaller ROCK1, and upregulation of the differentiation markers (Fig. 3A, lane 3). Similarly, retroviral transduction of keratinocytes with ICN1 gave rise to the smaller ROCK1 in association with MYPT1 phosphorylation (Fig. 2B, left panel). Of importance, confluence-triggered cell-cell contact also induced smaller ROCK1 and MYPT1 phosphorylation, indicating that the ligand-mediated NOTCH activation is responsible for these events (Fig. 2B, right panel). Assuming that activated NOTCH1 evokes some apoptotic cascade, ROCK activation may occur in parallel in cells undergoing apoptosis. However, we failed to detect any indication of apoptotic cell death after ICN1 transduction (Fig. 2C). To further corroborate involvement of NOTCH1 in ROCK1 activation, we knocked down NOTCH1 expression. In contrast to the control case, NOTCH1 silencing abrogated the production of the smaller

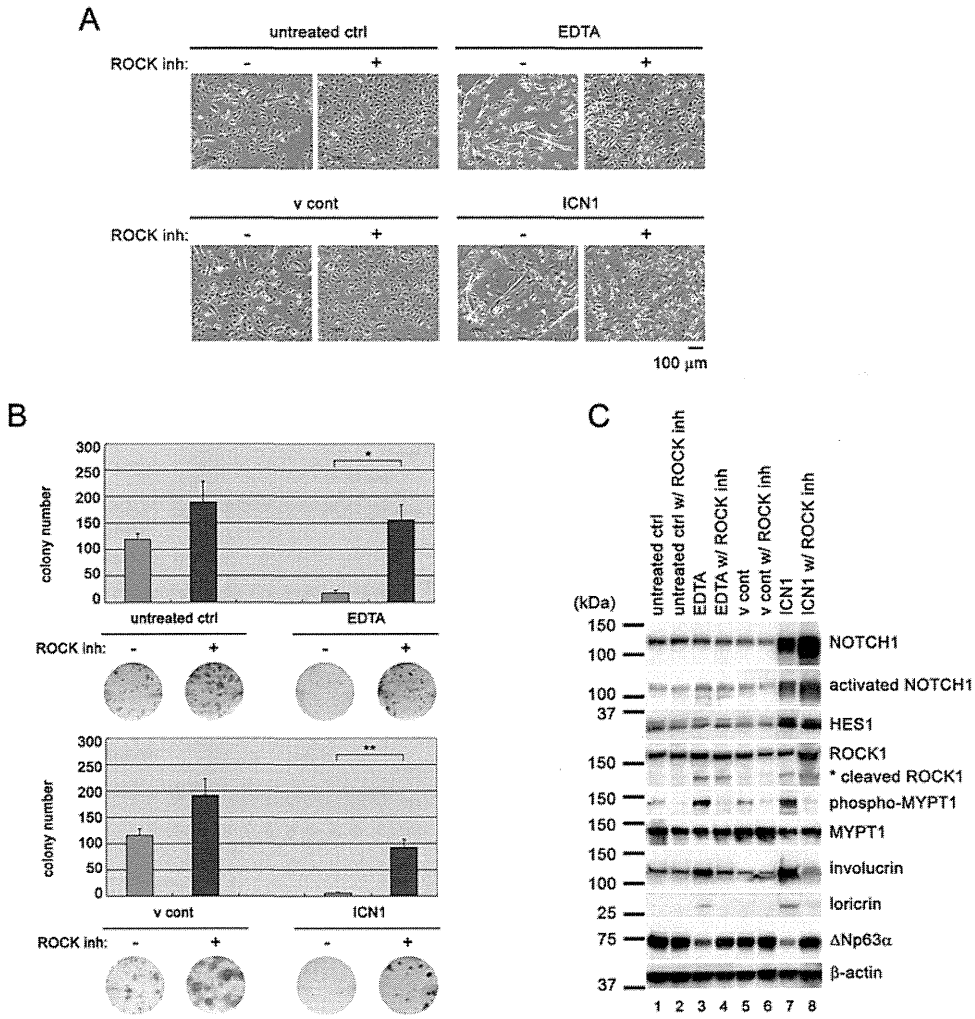

FIG 5 ROCK inhibition alleviates the growth-suppressive and differentiation-inducing effects of NOTCH1. (A) HCK1T cells pretreated with or without Y-27632 were either left untreated, treated with 2.5 mM EDTA, or transduced with ICN1 or vector control (v cont). Thereafter, cells were incubated in the presence or absence of Y-27632. Typical areas were photographed at 72 h after EDTA treatment. (B) Aliquots of 500 HCK1T cells were seeded on 35-mm dishes under sparse conditions. Cells pretreated with or without Y-27632 were then either left untreated, treated with 2.5 mM EDTA for 10 min, or transduced with ICN1 or vector control (v cont). After being cultivated for 2 weeks, the cells were stained with Giemsa's dye, and colonies were counted. The photographs are of representative dishes, and the graph represents means ± SDs. *, $P < 0.05$; **, $P < 0.01$ (according to Student's t tests). (C) Cells were treated similarly to those for panel A and incubated for 72 h. Cell extracts were subjected to immunoblotting analysis with the indicated antibodies.

ROCK1 and MYPT1 phosphorylation after differentiation stimuli (Fig. 3A) with restoration of clonogenic growth potential (Fig. 3B). Treatment with a γ-secretase inhibitor had the same effects as NOTCH1 knockdown (Fig. 4A and unpublished observations). These results suggest that the observed ROCK activation is not an outcome of apoptosis but is positively regulated by NOTCH1 signaling in differentiating cells.

The intracellular form of NOTCH is responsible for ROCK activation independently of its transcriptional activity. Given the immediate appearance of the smaller ROCK1 after expression of the intracellular NOTCH1, it can be hypothesized that NOTCH1 activation of ROCK1 does not occur through *de novo* protein expression. In an effort to clarify this, we treated cells with cycloheximide (CHX), an inhibitor of translation. While CHX treatment completely inhibited induction of the NOTCH1 transcriptional target, HES1, it did not affect the generation of the smaller ROCK1 and MYPT1 phosphorylation (Fig. 4A, upper panel, compare lanes 5 and 6). Since NOTCH1 requires the transcriptional coactivator, MAML1, in its transactivation complex, we also assessed the effect of dominant negative MAML1, MAML61-3HA. While exogenous expression of MAML61-3HA blocked the induction of HES1, it exerted no effect on the smaller ROCK1 production, MYPT1 phosphorylation, and expression of a differentiation marker, involucrin (Fig. 4B). It is still possible that the canonical NOTCH1 signaling plays a role in differentiation at a later stage, as the level of a terminal differentiation marker, loricrin, appeared to be attenuated to some extent in MAML61-3HA-expressing cells. To further explore the transcription-independent function of NOTCH1 in ROCK1 activation, we established tetracycline-inducible ICN1-ERT keratinocytes, expressing a chimeric protein consisting of the intracellular domain of NOTCH1 fused at the amino terminus to a mutated ligand-binding domain of the estrogen receptor (ERT) (57). In the presence of doxycycline (DOX) for 3 days and without addition of the

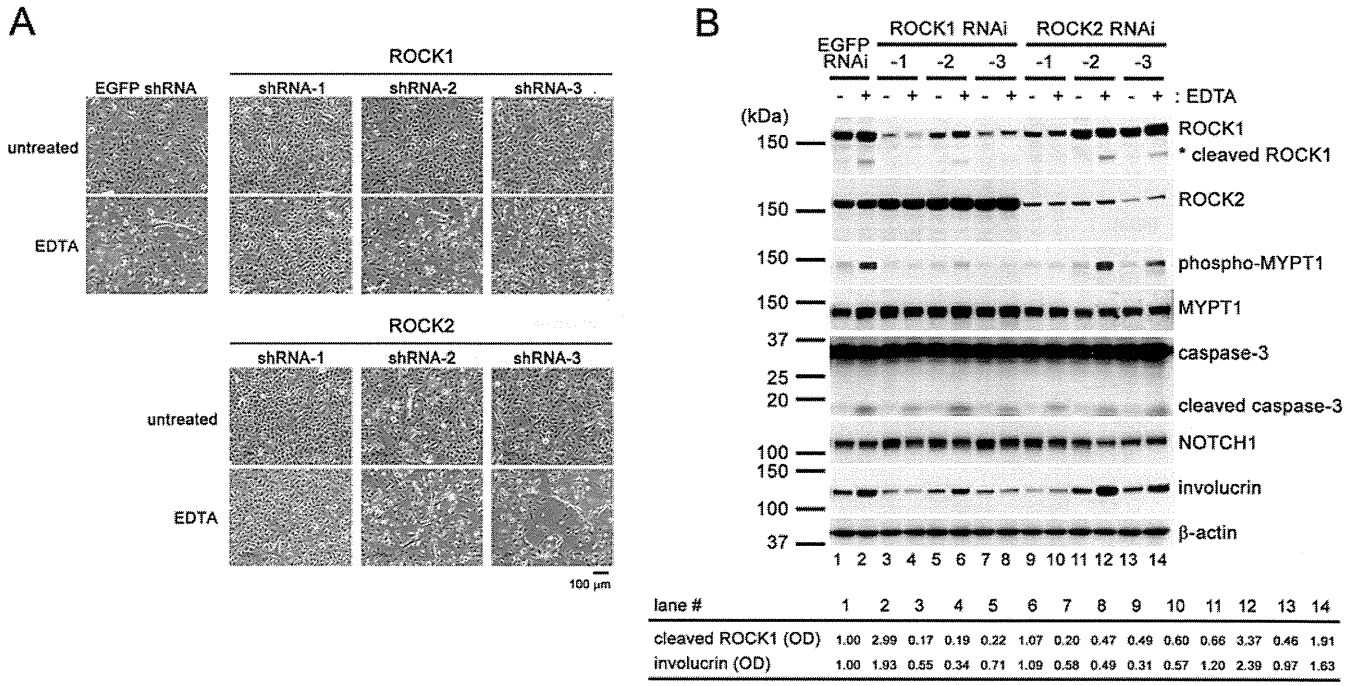

FIG 6 Knockdown of ROCK1 inhibits keratinocyte differentiation after EDTA treatment. (A) HCK1T cells stably transduced with shRNAs for ROCK1 and -2 were either left untreated or treated with 2.5 mM EDTA and then incubated with keratinocyte-SF medium. Typical areas were photographed at 3 days after EDTA treatment. Note that ROCK2 shRNA-2 knocked down ROCK1 expression as well. (B) HCK1T cells were transduced with three different shRNAs for ROCK1 and -2 or with control shRNA for EGFP. Cells were then either left untreated (−) or treated (+) with 2.5 mM EDTA for 10 min. After cultivation for 72 h, cells were harvested and analyzed by immunoblotting. The band optical densities (OD) for the cleaved ROCK1 and involucrin were quantified densitometrically, normalized to that of β-actin with the value for untreated control defined as 1.

estrogen homolog, ICN1-ERT did not transactivate the target gene but triggered the smaller ROCK1 production and MYPT1 phosphorylation (Fig. 4B, compare lanes 9 and 10). These results indicate a transcription-independent or cytoplasmic function of NOTCH1 in control of ROCK1 activity and its roles in cellular differentiation.

To elucidate whether the additional smaller fragment of ROCK1 is a constitutively active form generated by caspase-3-mediated cleavage (54, 55), cells were treated with the caspase inhibitor z-VAD prior to EDTA exposure. In the presence of active forms of NOTCH1, z-VAD markedly blocked generation of the smaller ROCK1 as well as MYPT1 phosphorylation (Fig. 4A, upper panel, compare lanes 5 and 7), indicating that the NOTCH intracellular form could induce immediate and constitutive activation of ROCK1 through caspase. This activation of caspase is much weaker than that observed in apoptotic cells, since cleavage of the well-known caspase substrate PARP was marginally detected only when pretreated with CHX (Fig. 4A lower panel), suggesting a nonapoptotic function of caspase activation in keratinocyte differentiation.

ROCK inhibition rescues the phenotype induced by NOTCH activation. Next, to address whether ROCK activation is the critical downstream event in NOTCH signaling, we tested whether the NOTCH gain-of-function phenotype could be reversed by ROCK inhibition. To this end, we assessed the differentiation status and clonogenic growth potential after EDTA treatment or ICN1 transduction in the presence of a ROCK inhibitor. ROCK inhibition significantly restored the morphology and clonogenicity of keratinocytes upon EDTA treatment or ICN1 transduction (Fig. 5A and B), and suppressed both induction of differentiation markers and reduction of ΔNp63α (Fig. 5C). Silencing of ROCK1 but not ROCK2 also blocked differentiation after EDTA treatment (Fig. 6A and B). Intriguingly, continuous ROCK inhibition rendered cells permissive to constitutive ICN1 expression as well as HES1 induction without indication of differentiation and maintained growth potential during at least three passages, while only cells expressing a small amount of ICN1 survived without the ROCK inhibitor (Fig. 7A). ROCK inhibition may allow increased NOTCH1 levels, possibly due to counterbalancing its biological effects. ROCK inhibitor withdrawal resulted in a prompt resumption of differentiation following MYPT1 phosphorylation in ICN1-expressing cells (Fig. 7B). These results suggest that ROCK is the critical downstream effector of NOTCH signaling in loss of stemness and differentiation of keratinocytes.

Ectopic expression of constitutively active ROCK1 induces keratinocyte differentiation. We next asked whether activated ROCK1 itself could initiate differentiation of normal human keratinocytes. For this purpose, we established several lines of keratinocytes expressing various exogenous ROCK1 mutants in a doxycycline-dependent manner. Upon induced expression of ROCK1ΔC241, a truncated mutant corresponding to a caspase-cleaved constitutively active form, downregulation of ΔNp63α and upregulation of a differentiation marker were evident to a level comparable to that observed in ICN1-ERT cells (Fig. 8A, compare lanes 2 and 8). Expression of wild-type ROCK1 exhibited only marginal effects (Fig. 8A, lane 6), while caspase-cleavage resistant ROCK1-D1113A and kinase-inactive ROCK1-K105A mutants failed to induce differentiation (Fig. 8A, lanes 10 and 12).

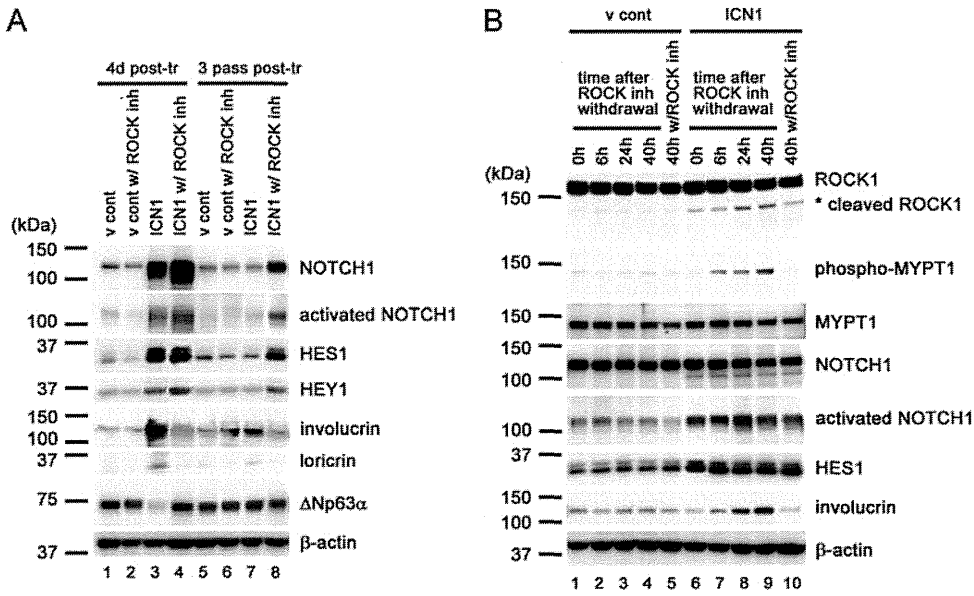

FIG 7 ROCK inhibition allows propagation of keratinocytes in the presence of constitutively active NOTCH1. (A) HCK1T cells pretreated with or without Y-27632 were transduced with the constitutively active form of NOTCH1 (ICN1) or vector control (v cont). Cells were cultivated until 22 days posttransduction (three passages) in the presence or absence of Y-27632. Cell extracts were prepared at 4 and 22 days posttransduction and subjected to immunoblotting analysis with the indicated antibodies. Note that the ROCK inhibitor inhibits differentiation and permits proliferation of ICN1-expressing cells. In contrast, control cells which have escaped after ICN1 transduction showed decreased levels of activated NOTCH1. (B) Cells were treated as for panel A. Cell lysates were prepared at the indicated time points after withdrawal of Y-27632 and subjected to immunoblotting analysis with the indicated antibodies.

It has been shown that the Rho inhibitor C3 as well as Y-27632 inhibited differentiation induced by single-cell suspension, although RhoA activity is unvaried during differentiation (35). In our monolayer culture model, conditional overexpression of a constitutively active form of RhoA was able to promote differentiation to some extent (Fig. 8B, lane 2). We then examined C3's effect on the process of keratinocyte differentiation. C3 only partially inhibited overall ROCK activation, judging from the phosphorylation levels of MYPT1 (Fig. 8C, compare lanes 2 and 7). Furthermore, this inhibition seemed to be closely associated with unexpected inhibition of the NOTCH1-caspase-ROCK1 axis through unknown mechanisms. Therefore, unlike keratinocyte differentiation induced by single-cell suspension assays, ROCK1 activation in monolayer culture essentially depends on its cleavage by caspase but not much on Rho activation, though we have not confirmed Rho activity during keratinocyte differentiation. These data support the conclusion that the NOTCH1-caspase-ROCK1 axis plays a major role in keratinocyte differentiation at least in monolayer culture. It is noteworthy that ROCK1 acts downstream of NOTCH1 but not NOTCH2, as ICN2 (a NOTCH2 intracellular form) did not induce ROCK1 cleavage and keratinocyte differentiation (Fig. 8A, compare lanes 2 and 4).

Proliferative defects upon dissociation in hiPSCs are partly attributable to NOTCH activity. It is well-known that human pluripotent stem cells such as hESCs undergo massive apoptosis when dissociated and that ROCK inhibitor treatment efficiently ameliorates such vulnerability to permit survival in clonal culture (39, 58). It is tempting to speculate that the NOTCH-ROCK pathway may also be activated in human pluripotent stem cells during the dissociation step with EDTA treatment and that this could be one mechanism underlying dissociation-induced loss of clonal growth potential. In an attempt to assess this possibility, we employed two lines of human induced pluripotent stem cells (hiPSCs). As shown in Fig. 9A and B, virtually no hiPSC colonies were formed from cells dissociated by trypsin-EDTA treatment, whereas NOTCH inhibition by a γ-secretase inhibitor partially restored the efficiency of colony formation to a degree comparable to that with Rho inhibitor C3-treated cells. Combination inhibition of γ-secretase and Rho had an additive effect on the clonogenic growth capacity to the same extent as ROCK inhibition, suggesting that the NOTCH-ROCK and the Rho-ROCK axis act in parallel in this cellular context.

In line with a previous study showing ROCK-dependent myosin activation as the direct cause of dissociation-induced cell death in hESCs (41), we also found that treatment with the myosin inhibitor blebbistatin showed equal efficacy as ROCK inhibition (Fig. 9C and D).

To substantiate further the link between NOTCH and ROCK in hiPSCs, we next assessed the status of NOTCH and ROCK in adherent small clumps of cells treated with EDTA. In accordance with the data with keratinocytes, EDTA treatment triggered immediate NOTCH1 activation accompanied by ROCK1 cleavage and MYPT1 phosphorylation (Fig. 10A, lanes 2 and 6). Importantly, treatment with a γ-secretase inhibitor resulted in abrogation of ROCK1 activation (Fig. 10A, lanes 4 and 8), suggesting that regulation of ROCK1 activity by NOTCH1 is also conserved in hiPSCs. Because EDTA treatment instigated drastic morphological change which was blocked by NOTCH or ROCK inhibition (Fig. 10B), we speculated that this stimulus may have an impact on the cell fate. Indeed, 3 days after EDTA treatment, expression of the stemness marker OCT3/4 was substantially downregulated in still-attached control cells (Fig. 10C, compare lanes 7 and 8). In-

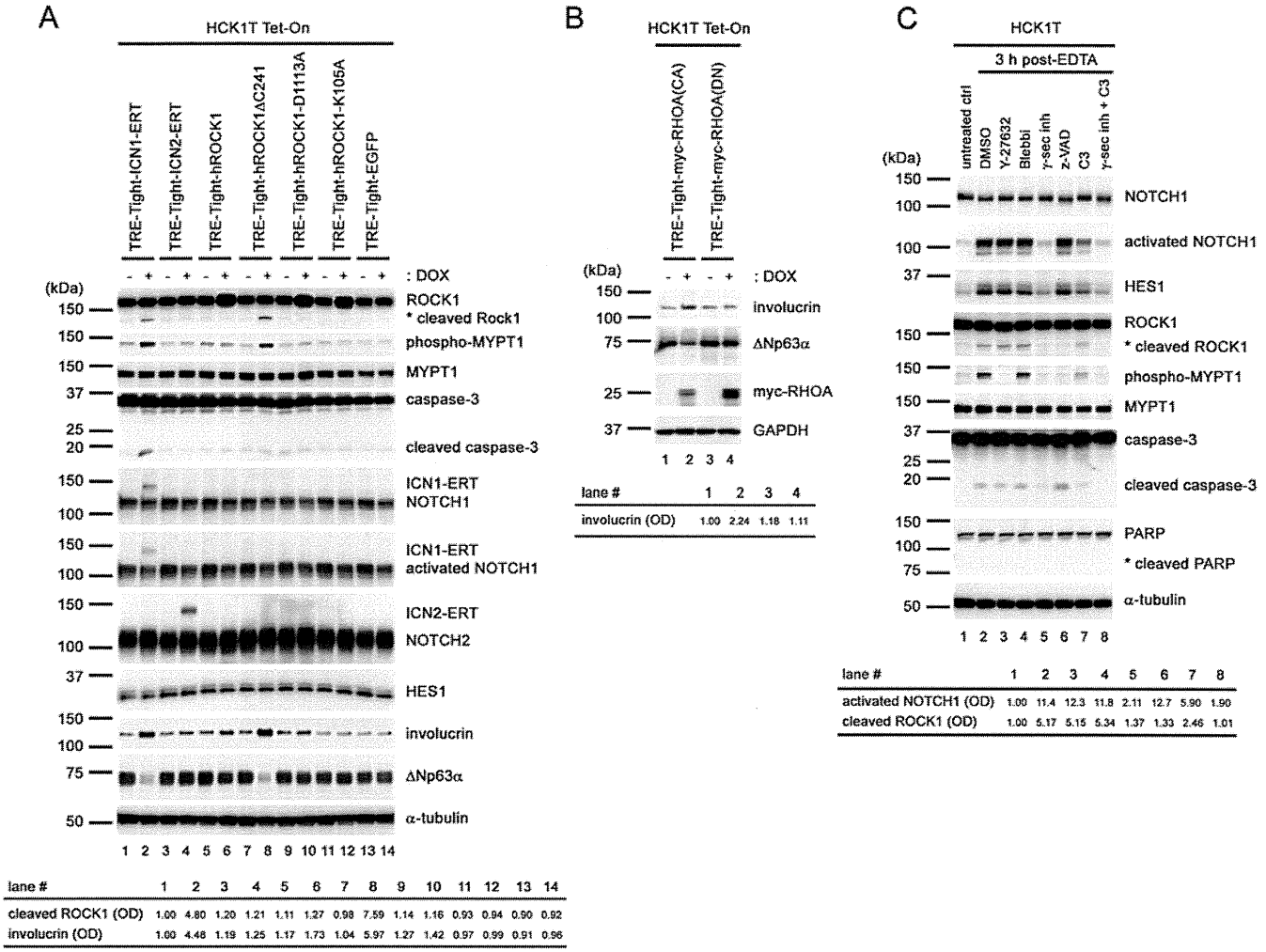

FIG 8 Ectopic expression of active ROCK1 induces keratinocyte differentiation. (A and B) HCK1T Tet-On cells were stably transduced with the indicated tetracycline-inducible gene constructs by retroviral gene transfer. Cells were either left untreated (−) or treated (+) with 1 μg/ml doxycycline (DOX) for 72 h. Cell extracts were analyzed by immunoblotting with the indicated antibodies. A long-exposed image for activated NOTCH1 is shown. Quantification of relative optical densities (OD) for the cleaved ROCK1 and involucrin bands, normalized to the value for the α-tubulin or GAPDH control, are indicated. (C) HCK1T cells, pretreated where indicated with 10 μM Y-27632, 10 μM blebbistatin, 10 μM γ-secretase inhibitor (DAPT), 20 μM z-VAD-fmk, or 1.0 μg/ml C3 for 3 h, were either left untreated or treated with 2.5 mM EDTA for 10 min and incubated with keratinocyte-SF medium for 3 h. Cell extracts were subjected to immunoblotting analysis with the indicated antibodies. Quantification of relative optical densities (OD) for the activated NOTCH1 and cleaved ROCK1 bands, normalized to the value for α-tubulin with the untreated control defined as 1, are indicated.

hibition of either NOTCH or Rho significantly prevented this transition (Fig. 10C). Of note, the inhibitor-treated colonies showed normal morphology in a mass, whereas the EDTA-treated controls exhibited heterogeneous and differentiated traits at this time point. These observations indicate that EDTA treatment induces acute ROCK1 activation and consequent loss of stemness at least partly in a NOTCH-dependent manner in hiPSCs.

DISCUSSION

Identification of NOTCH1 as a novel upstream regulator for ROCK1. The best-known upstream regulator for ROCK activity is Rho GTPase (32). In the normal cellular context, ROCK becomes an active kinase by conformational change through interaction with the GTP-bound form of Rho, which is thought to release the kinase domain from the carboxy-terminal autoinhibitory domain. In apoptotic cells, removal of the autoinhibitory domain of ROCK1 by caspase-3-mediated cleavage renders this protein constitutively active (54, 55, 59). In the present study, we first found that the cleaved ROCK1 is also generated immediately after emergence of the NOTCH1 intracellular form in the context of keratinocyte differentiation and revealed that activated NOTCH1 causes constitutive activation of ROCK1 through caspase cleavage upon EDTA treatment or exposure to differentiation-inducing stimuli such as serum as well as cell-cell contact (Fig. 11). We further demonstrated that this type of ROCK1 activation is mediated by a transcription-independent function of NOTCH1. Thus, we conclude that noncanonical NOTCH1 signaling triggers differentiation and a consequential decrease in clonogenicity mostly if not completely through ROCK1 activation in keratinocytes. To our knowledge, this is the first demonstration of NOTCH1 function as a novel and critical upstream regulator for ROCK1 activity. The Rho inhibitor C3 inhibited MYPT1 phosphorylation to some extent in concert with reduction of activated NOTCH1 and